A SURVEY OF GALAXY REDSHIFTS. II. THE LARGE SCALE SPACE DISTRIBUTION

MARC DAVIS, JOHN HUCHRA, DAVID W. LATHAM, AND JOHN TONRY
Harvard-Smithsonian Center for Astrophysics
Received 1981 May 14; accepted 1981 August 17

ABSTRACT

We have finished a redshift survey of galaxies complete to 14.5 m_B in the north and south galactic polar caps above declination $=0°$ and containing some 2400 galaxies. We present here various projections of the resulting redshift-space maps. While different in detail, the statistical nature of the redshift-space distribution is very similar between the north and south. The space distribution of galaxies is frothy, characterized by large filamentary superclusters of up to 60 Mpc in extent, and corresponding large holes devoid of galaxies. We also present redshift-space maps generated from n-body simulations, which very roughly match the density and amplitude of the galaxy clustering but fail to match the frothy nature of the actual distribution. Our results present a severe challenge to all theories of galaxy and cluster formation.

Subject headings: cosmology — galaxies: clusters of — galaxies: redshifts

I. INTRODUCTION

For the past several years we have endeavored at the Center for Astrophysics (CfA) to complete a moderately deep, wide angle redshift survey of nearby galaxies. Our goal has been to obtain a complete data set in order to pursue a host of cosmological studies, such as determinations of the cosmological density parameter Ω, the study of the nature of the galaxy covariance function $\xi(r)$, and the nature of large scale clustering.

We chose to restrict ourselves to galaxies listed by Zwicky *et al.* (1961) with $m_B \leq 14.5$, $\delta \geq 0$, and $b^{II} \geq 40°$ or $b^{II} \leq -30°$. This sample reaches well beyond the local (Virgo) supercluster, and is not severely disturbed by galactic absorption. It was hoped that the volume of space we surveyed would begin to approximate a fair sample volume of the universe. The CfA survey is complementary to other new redshift surveys which generally drill smaller patches of the sky to deeper limits (cf. Kirshner, Oemler, and Schechter 1979; Gregory, Thompson, and Tifft 1981; Tarenghi *et al.* 1979, 1980; Gregory and Thompson 1978; Ellis *et al.* 1981; Tifft 1980). These previous surveys have demonstrated the existence of superclusters and holes 20–30h^{-1} Mpc in size and have hinted at the existence of larger scale filaments and lumps. Sandage (1978) has published redshifts for the Shapley-Ames catalog, which is nearly complete to magnitude $\sim$13.0 over the entire sky (12.7 in the B_T magnitude system). Tully and Fisher (1981) have recently released their catalog of 21 cm redshifts of late-type galaxies with diameter $\geq 2'$ and $v < 3000$ km s^{-1}, $\delta > -45$. The list is almost complete for late spiral galaxies with $\delta > 0$. Of course there have been many redshifts obtained by a host of authors for a

variety of reasons. We have compiled all the published redshifts into a massive catalog; we have reobserved only those galaxies in our sample space which previously had poor velocity determinations. An excellent inter-comparison of observers' errors is given by Rood (1981). Objects listed as "double" or "multiple" in Zwicky *et al.* (1961) have had magnitudes assigned to the individual components based on their combined magnitude and estimates (by J. H.) of their relative brightness and have only been observed when the individual components fit the sample definition.

Our survey covers 2.7 sr, and the mean redshift is roughly 5000 km s^{-1}. The sample in the north galactic cap contains 1874 galaxies, for which we now have redshifts of all but one. The south galactic cap that we sample contains 569 objects, and redshifts are now available for all but six. The remaining galaxies are mostly low surface brightness dwarfs and irregulars.

All data were obtained using a photon-counting Reticon detector and intermediate-dispersion spectrograph (the Z-machine) on the Mount Hopkins 1.5 m telescope. The characteristics of an early version of the detector have been described by Davis and Latham (1979), although many important improvements have been incorporated in the past two years. Details of the data analysis technique are given by Tonry and Davis (1978, hereafter Paper I; 1981a) and by Tonry (1980). According to Rood (1981), our typical external redshift error is ± 37 km s^{-1}, which agrees well with our internal error estimates. Our redshift catalogs are still in preparation and will be published elsewhere.

In this paper we present a series of redshift-space maps of the observed galaxy distribution and compare them to similar projections made from 20,000 point
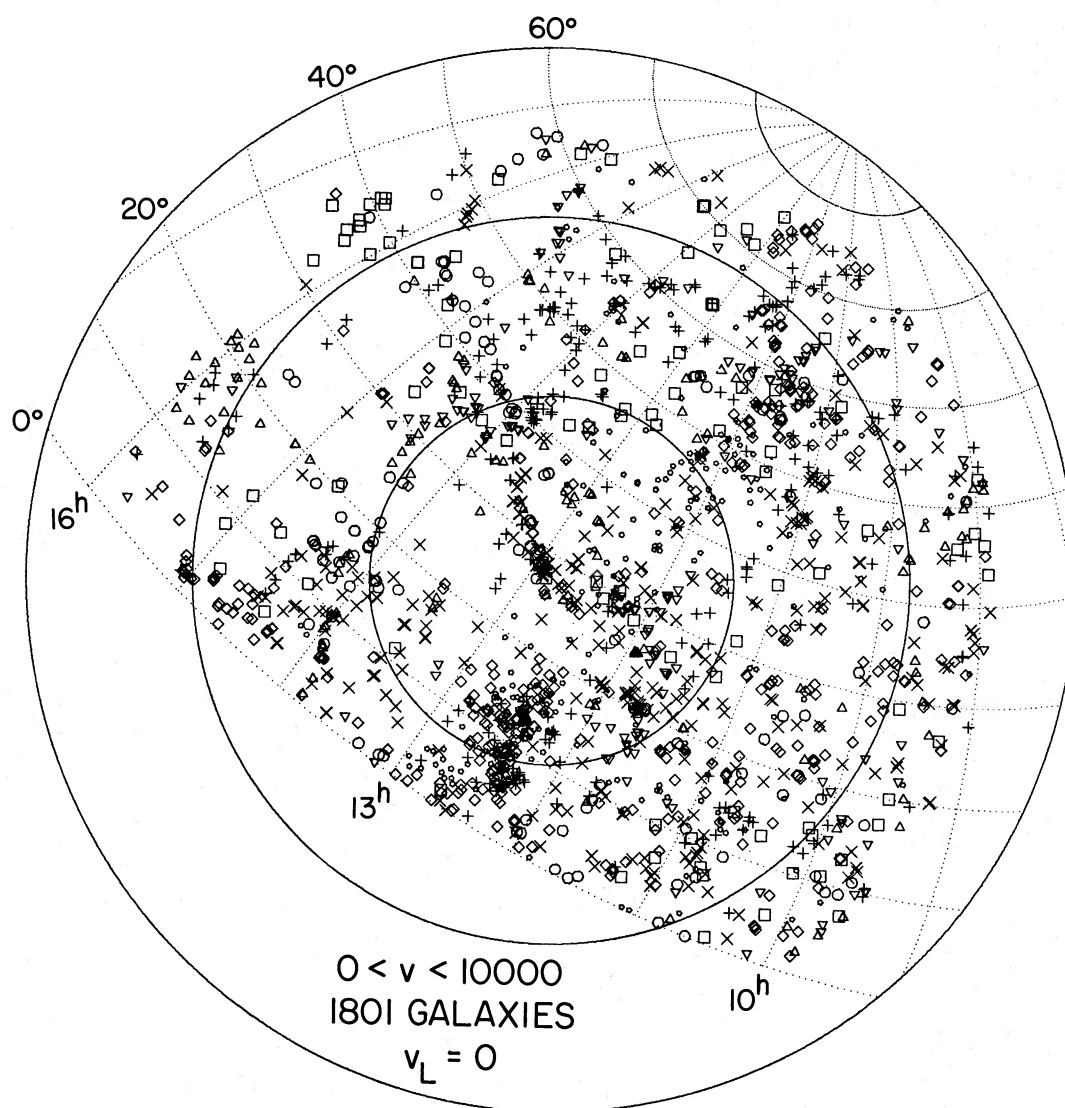
FIG. 1a.—The 14.5 mag north survey displayed in an equal area galactic coordinate frame. The galactic pole is at the center, and the circles denote galactic latitude 70°, 50°, and 30°. The dotted curves are lines of constant declination and right ascension. All objects with galactocentric velocity $0 < v < 10,000$ km s^{-1} are plotted. No luminosity selection is applied here. The various symbols denote velocity bins as follows: pentagons are $0 < v < 1000$; diamonds are $1000 < v < 2000$; plus signs are $2000 < v < 3000$; inverted triangles are $3000 < v < 4000$; triangles are $4000 < v < 5000$; circles are $5000 < v < 6000$; (X's) are $6000 < v < 8000$; and squares are $8000 < v < 10,000$.

n-body simulations of Efstathiou and Eastwood (1981). The accuracy of the Zwicky magnitudes does not affect the present discussion. Dynamical analyses, density studies, and studies of luminosity functions will be discussed in future papers. Our purpose here is to describe the interesting features of the overall distributions and to compare the observations to the expectations of various cosmogonic scenarios.

II. THE MAPS

Figures 1a and 1b show the complete 14.5 mag survey projected onto galactic coordinates. The north galactic

cap is shown in Figure 1a and the south galactic cap in Figure 1b. The northern sample is limited to $\delta \geq 0$, $b \geq 40$, or 1.83 sr, while the southern section is bounded by $b \leq -30$, and $\delta \geq -2.5$, the southern boundary of the Zwicky catalog. The southern region encloses 0.83 sr. The various symbols represent different velocity windows, as indicated. All velocities have been corrected for 300 km s^{-1} galactic rotation, and objects with recessional velocity greater than 10,000 km s^{-1} or less than 0 are not plotted.

The most prominent features in the north are the Virgo cluster center (at 12^h5, $+12°$) and the Coma cluster core (at 13^h, $+29°$). The supergalactic plane
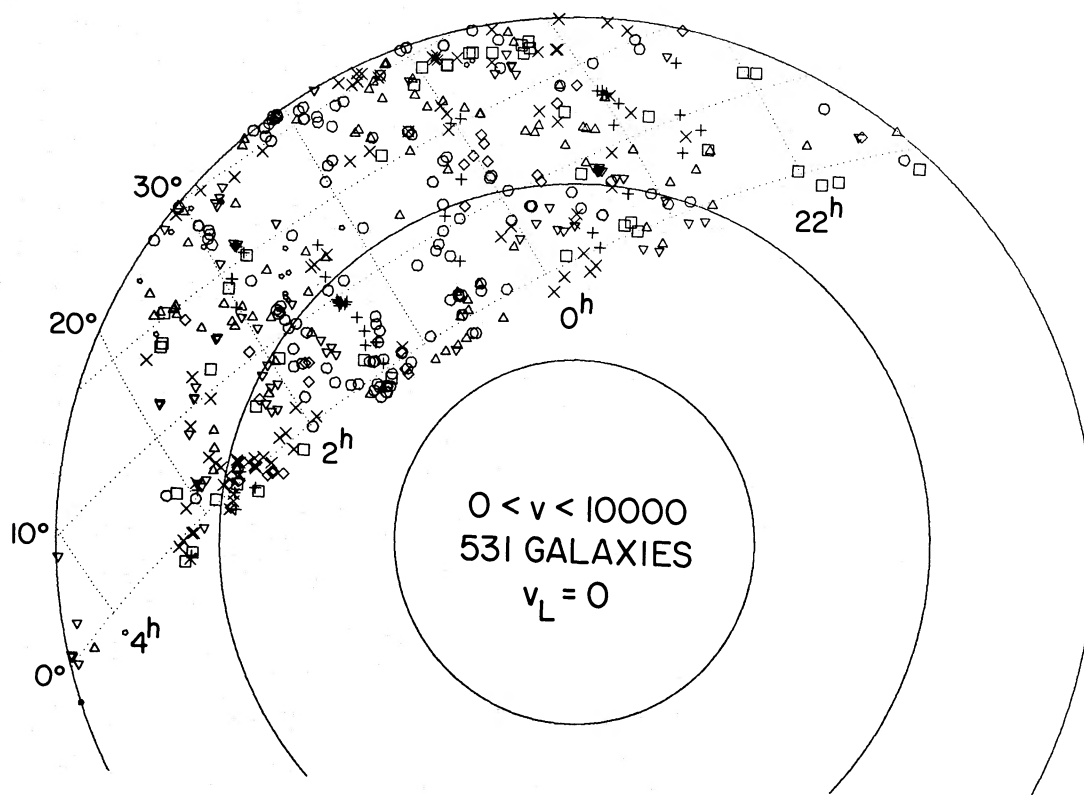
FIG. 1b.—The southern galactic cap survey, plotted as in Fig. 1a. The absence of galaxies in the 3^h region is largely due to galactic obscuration.

extending from Virgo to Ursa Major (at 11^h6, $+58°$) is not nearly as prominent here as in the brighter, more limited Shapley-Ames sample. There are no features that dominate strongly in the southern slice.

To obtain a clearer view of the clustering, we divided the samples into three redshift windows. Since our survey is magnitude limited, the farthest window only picks out the most luminous galaxies, while the nearest window includes a host of low luminosity objects. Thus, when all the galaxies in the survey are retained, the nearest clusters appear artificially richer than the more distant clusters. We have tried to soften this selection effect in the maps shown in Figures 2 and 3 by deleting all galaxies that are not luminous enough to be seen out to a redshift distance of 4000 km s^{-1} ($M \leq -18.5$ for $H_0 = 100$ km s^{-1} Mpc^{-1}). The choice of 4000 km s^{-1} is a compromise; if we had used 10,000 km s^{-1} to produce true volume-limited selection with the same luminosity cutoff for all three windows, then only 6% of the galaxies in the survey would have survived. When calculating a galaxy's luminosity, to see if it passed the 4000 km s^{-1} cutoff, we included a correction for the "infall" toward Virgo, using a spherically symmetric flow model scaled to an infall of 440 km s^{-1} for the Local Group (Tonry and Davis 1981b). Furthermore, every galaxy

within 6° of the Virgo center and with velocity less than 2500 km s^{-1} was assumed for the sake of the luminosity calculation to be at the velocity of the Virgo core, 1460 km s^{-1}. However, the velocities plotted in Figures 2 and 3 have not been corrected for the Virgo flow in order to keep the maps as close to the direct observations as possible. Figures 2a, 2b, and 2c detail the northern catalog when selected in this fashion for the observed velocity ranges $0 < v < 3000$ km s^{-1}, $3000 < v < 6000$ km s^{-1}, and $6000 < v < 10,000$ km s^{-1}. Figures 3a, 3b, and 3c apply the same selection to the southern slice. Note that Figures 2a and 3a show true volume-limited samples, while the others do not.

For the nearest redshift window, the 4000 km s^{-1} luminosity cutoff divides the sample approximately in half. Figures 2a and 2d show the nearest northern galaxies brighter and fainter than the cutoff. In both figures, the Virgo cluster complex and Ursa Major cloud stand out prominently, and in general the clustering is remarkably similar in the two pictures. The most obvious difference is some filling in of the supergalactic plane between Virgo and Ursa Major with nearby low-luminosity galaxies. However, this sample is not properly volume-limited, and Figure 2a gives a much fairer picture of the highly clumped nature of the supergalaxy
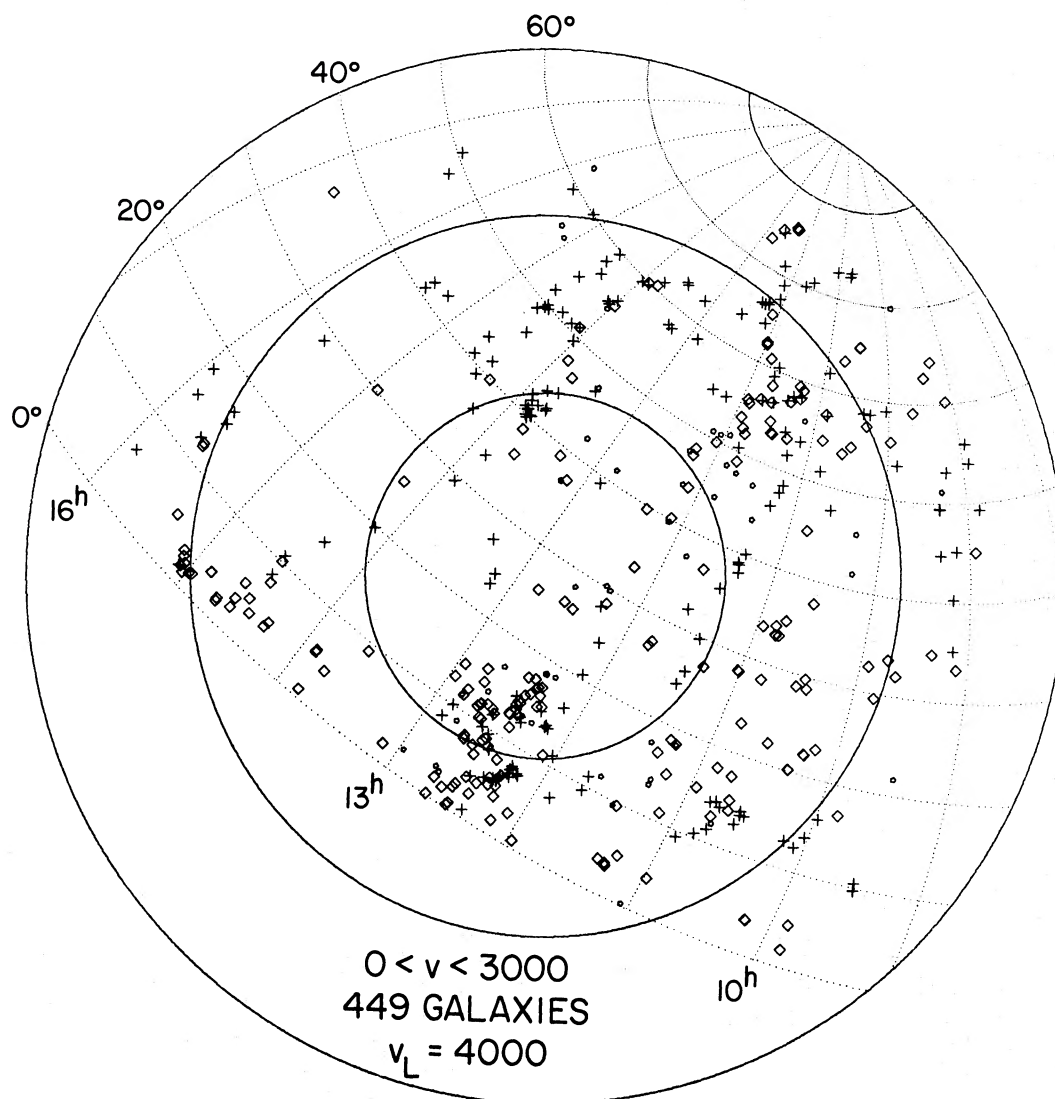
FIG. 2a.—A subset of Fig. 1a, in which are plotted galaxies in the velocity range $0 < v < 3000$ km s^{-1}, each of which is luminous enough to be observable to a minimum velocity of 4000 km s^{-1} ($M < -18.5$). The symbols are the same as in Fig. 1a.

and the obvious asymmetries above and below the supergalactic plane. Perhaps the most striking asymmetry is between the north and south, Figures 2a and 3a. Per unit area, there are seven times more galaxies in our northern sample than our southern slice. Since both these samples are essentially volume-limited, the same factor applies per unit volume. There is a remarkable hole, almost void of galaxies, in this part of the south galactic cap. Clearly the assumption that Virgocentric velocity fields can be calculated from spherically symmetric models with a uniform background is only a first approximation, incorrect in detail (Davis and Huchra 1981).

The intermediate and distant redshift windows, shown in Figures 2b, 3b, 2c, and 3c, exhibit clustering in

frothy, almost filamentary, patterns of connectedness surrounding empty holes on the sky. Although these samples are not properly volume limited, the selection effects should not invalidate direct comparisons of the corresponding northern and southern pictures. In sharp contrast to the nearby hole in the south, the middle window has more galaxies per unit area in the south than its northern counterpart, while the north is again richer in the most distant window.

Transverse views of the redshift-space maps are shown in Figures 4 and 5, where we plot right ascension versus velocity for various declination wedges. Once again, low luminosity galaxies have been eliminated, so all these pictures are volume-limited to a distance of 4000 km s^{-1} and magnitude-limited beyond.
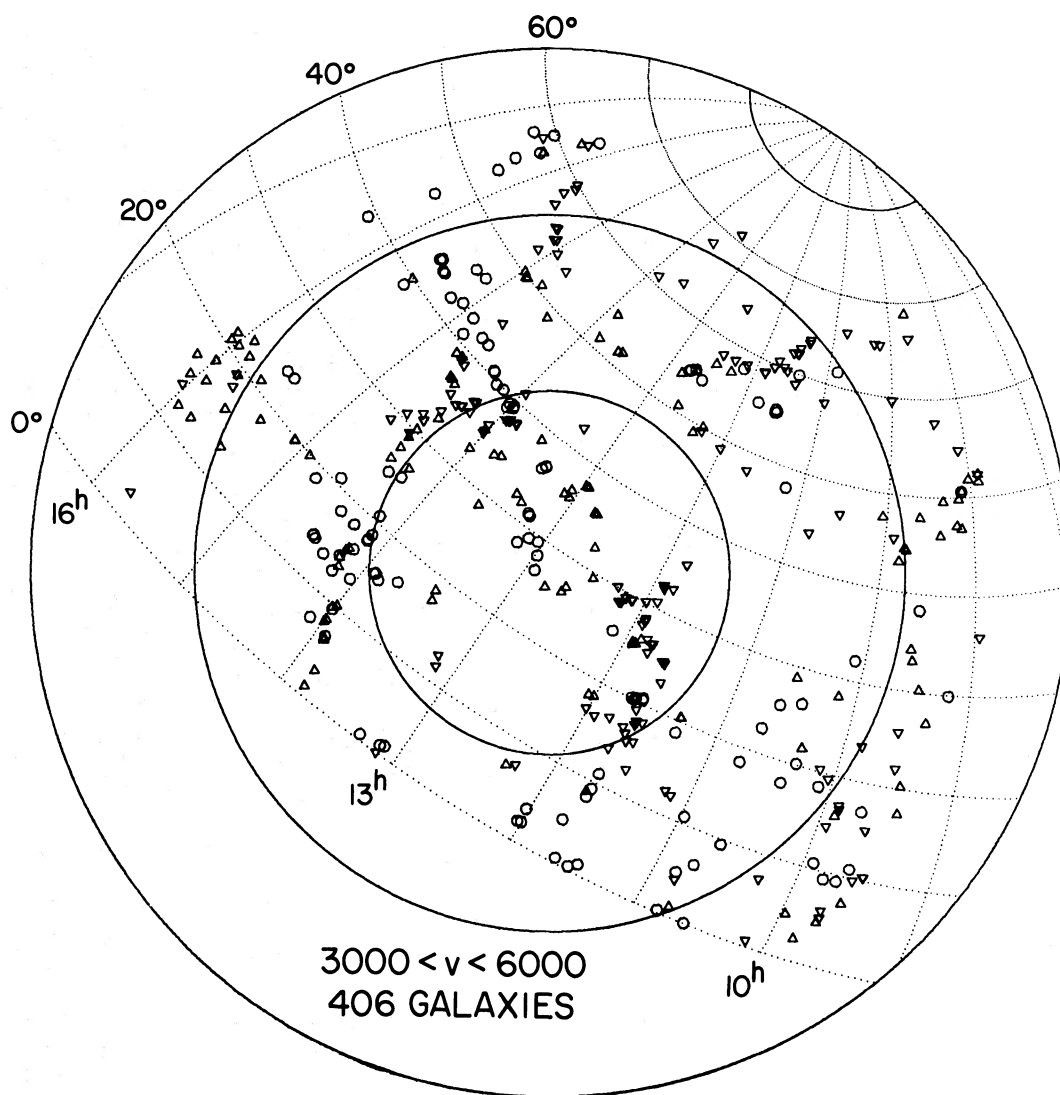
FIG. 2b.—Same as Fig. 2a for galaxies in the range $3000 < v < 6000$ km s^{-1}, again selecting only objects with $M < -18.5$

The transverse maps confirm the general impression that the large scale clustering is characterized by connected features surrounding large holes often 20 Mpc or more across, both in the north and the south. Some of the large scale features deserve specific mention here, although detailed discussion is postponed for future papers.

a) The Local Supercluster

The major components of the Local supercluster show up prominently in Figures 4a and 4b. The Virgo cluster itself is a complex smear of galaxies covering an hour of right ascension between 12^h and 13^h and extending from -500 to 2500 km s^{-1}. Even on these relatively crude

maps, there is a suggestion of several main subgroups, each at a substantially different redshift.

Only within the 6° circle centered on the Virgo core do we encounter luminous galaxies with negative redshift. None of the negative velocity galaxies are plotted in Figures 1–5, and of the 12 galaxies in the Virgo core with $v < 0$, seven are more luminous than $M = -18.5$. The various groups and subclusters within the supercluster such as the Virgo E, Virgo S, Virgo S', Virgo W, Ursa Major I, Leo II, and Virgo III clouds are all clearly identifiable (cf. de Vaucouleurs and de Vaucouleurs 1973). The Virgo region is sufficiently complex and subclustered that the assignment of a mean redshift for the entire Virgo supercluster center is not trivial, and yet is extremely important for cosmological tests of Virgocentric infall.
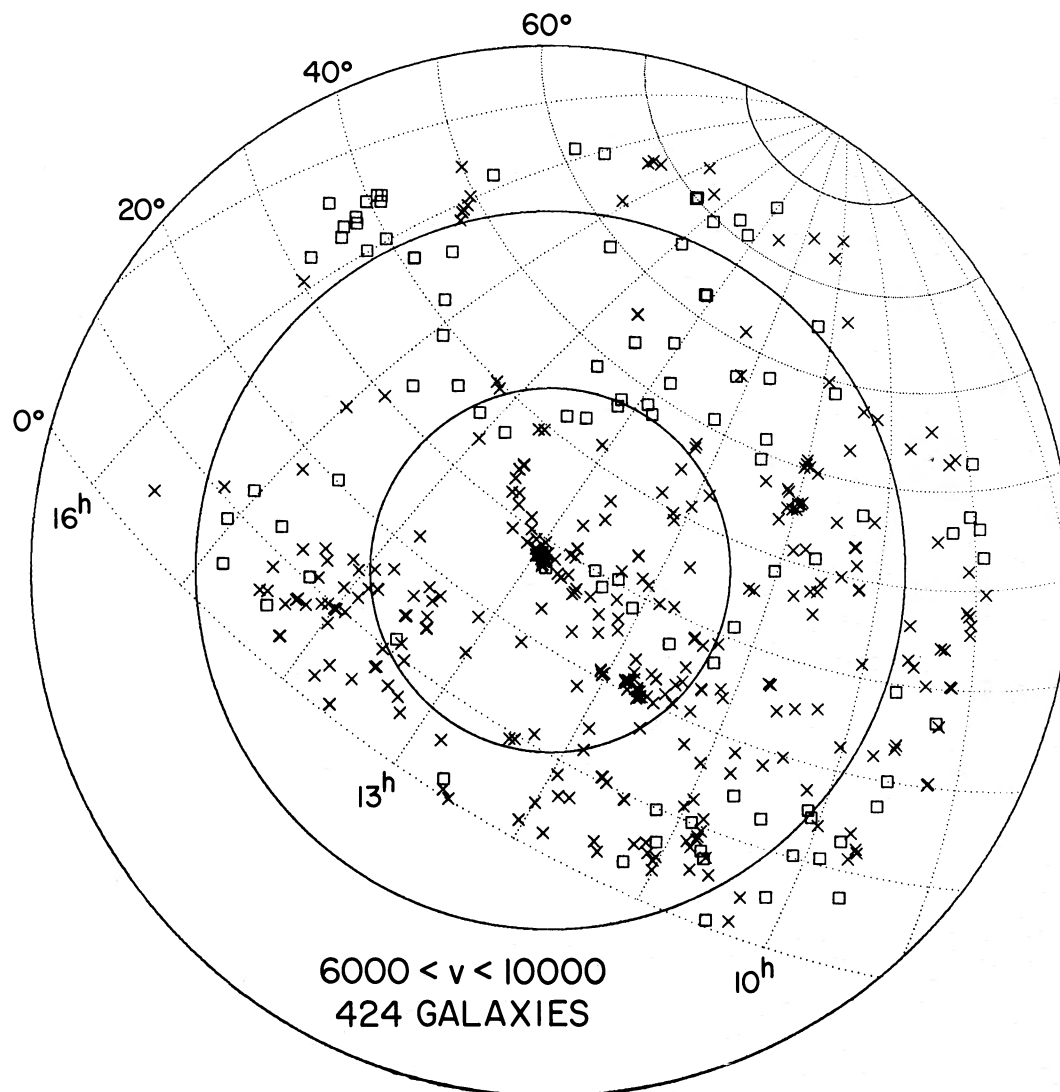
FIG. 2c.—Same as Fig. 2a for galaxies in the range $6000 < v < 10{,}000$ km s^{-1}. This section is completely magnitude limited.

b) Other Abell Clusters

The Abell 1367 cluster (11^h7, $+21°$, $+6700$ km s^{-1}) and the Coma cluster (12^h9, $+29°$, 7000 km s^{-1}) are quite prominent in Figures 2c and 4c and form two centers of a very extended prolate supercluster stretching from ($11^h +20°$, 6000 km s^{-1}) to ($14^h +40°$, 8000 km s^{-1}), which is a spatial extent of nearly 60 Mpc but a thickness along the two short axes of only ~ 10 Mpc. Although this supercluster appears to extend to Abell 2197/2199 complex (16^h3, $+38°$, 9500 km s^{-1}), a detailed examination of Figure 4d shows a gap of 15 Mpc separating the two. The N5416 group does *not* appear to be a part of the Coma supercluster (Thompson Wellier, and Gregory 1978; Chincarini Hayes, and Giovanelli 1979). Only in the rich cluster centers Virgo, A1367, and

Coma does the velocity dispersion of the galaxies distort the distribution into an obvious elongated cigar (a "finger of God" pointing toward the observer).

In the southern sample, Abell 194 (1^h4, $-1°$, 5500 km s^{-1}) and Abell 400 (2^h6, $+0°$, 6500 km s^{-1}) are both prominent and form part of a nearly continuous region of high density that includes additional clusters at (0^h5, $+3°$, 5500 km s^{-1}) and (1^h7, $+12°$, 5300 km s^{-1}) and extends northward to clusters at (1^h1, $+32°$, 5200 km s^{-1}) and (2^h0, $+25°$, 5100 km s^{-1}). It is quite remarkable how much of the clustering in the southern slice is concentrated around 5500 km s^{-1}, the redshift of the Perseus cluster nearly 40° away in the sky. The redshift elongation of these southern clusters is not as pronounced as in the A1367/Coma clusters, presumably because they are not as rich as the northern
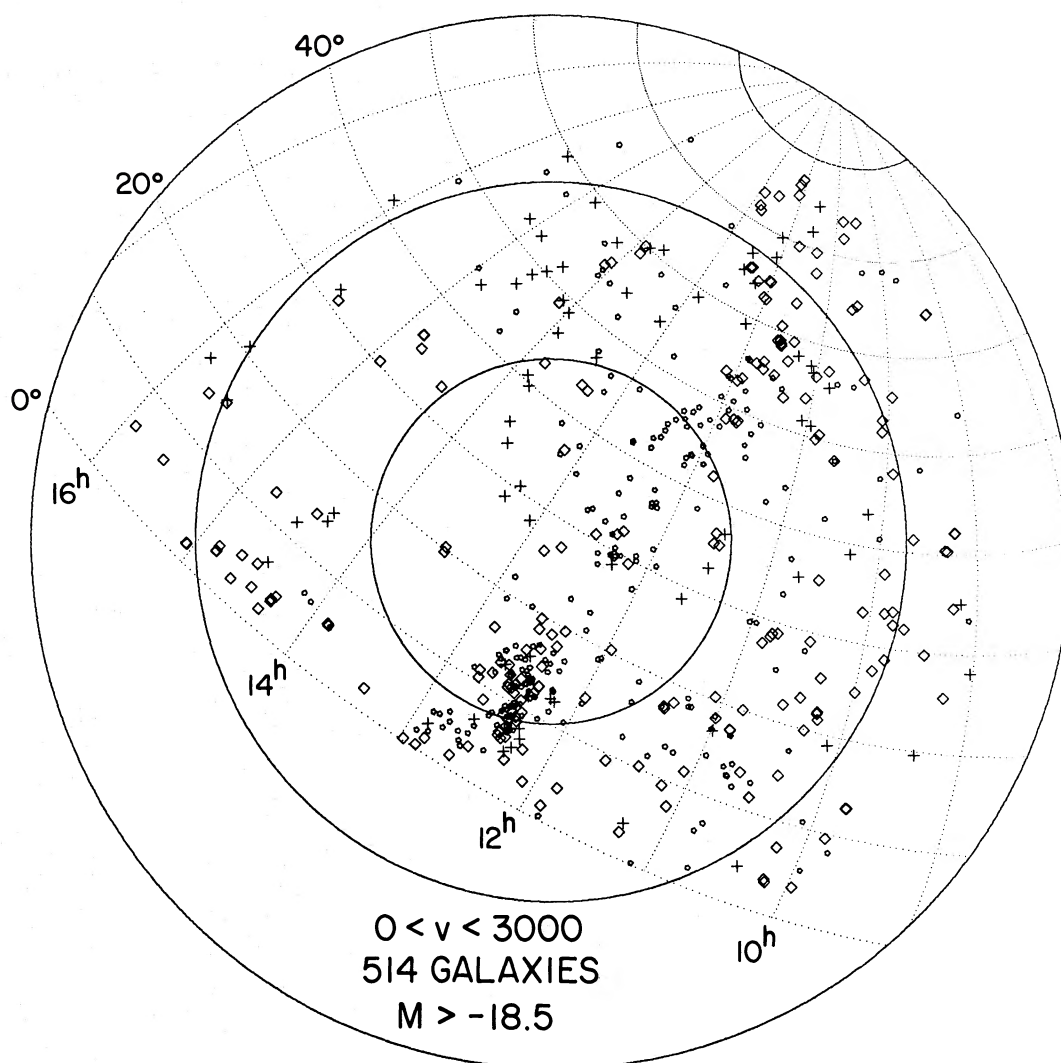
FIG. 2d.—Same as Fig. 2a for galaxies in the range $0 < v < 3000$ km s^{-1} and now with $M > -18.5$. Compare this to the bright galaxies plotted in Fig. 2a.

Abell clusters and so have lower dispersions and lower contrast to define the fingering.

The overall distribution of these clusters at 5000–6000 km s^{-1} is somewhat amorphous, with dimensions very roughly of 30×30 Mpc projected onto the sky with a redshift thickness of ~ 20 Mpc. The overall system is thus very slightly oblate.

Many of the nearby Zwicky clusters listed by Zwicky *et al.* (1961) can be identified within these maps, but the listed clusters are generally confined to much smaller scales, denoting the densest regions of clustering, and not the very large scale structure evident in our maps.

c) The Large Scale Structure

The nature of the large scale clustering defies a simple qualitative description. The overall distribution has a

hierarchical quality about it, as for example, seen in the A1367/Coma clusters which form an elongated supercluster composed of several subgroups. The intermediate velocity zone, $3000 < v < 6000$ km s^{-1}, is very underdense relative to the near and far zones in the north, while exactly the opposite is true in the south, so that there is considerable coherence to the fluctuations with a scale length of at least 30 Mpc. The north intermediate zone shown in Figure 2b is itself comprised largely of loosely defined clouds of typical diameter $10°$, or ~ 8 Mpc, which show little elongation in redshift space. Although the individual groups of the intermediate zone appear to have a filamentary connected structure, it could just as well be a random projection of several independent groups. There are many clusters, the majority in fact, throughout the sample of volume, that have
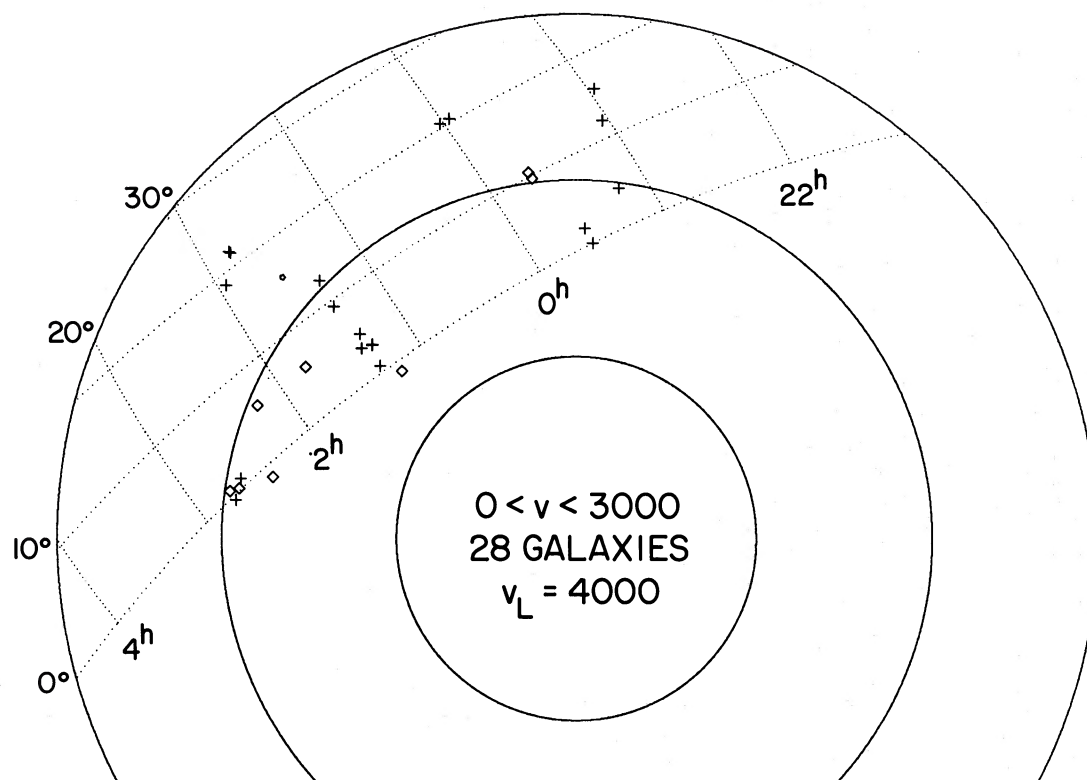
FIG. 3a.—A subset of the southern cap projections, showing galaxies in the range $0 < v < 3000$ km s^{-1} and $M < -18.5$
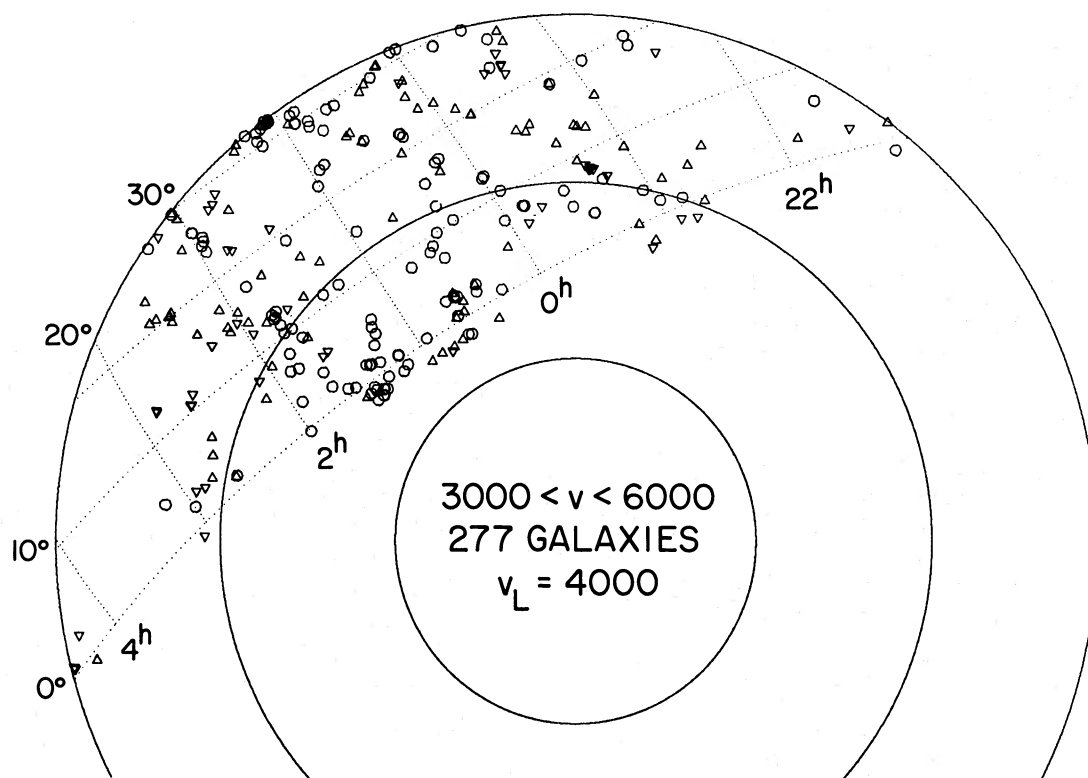

FIG. 3b.—Same as Fig. 3a for galaxies in the range $3000 < v < 6000$ km s^{-1} and $M < -18.5$

430
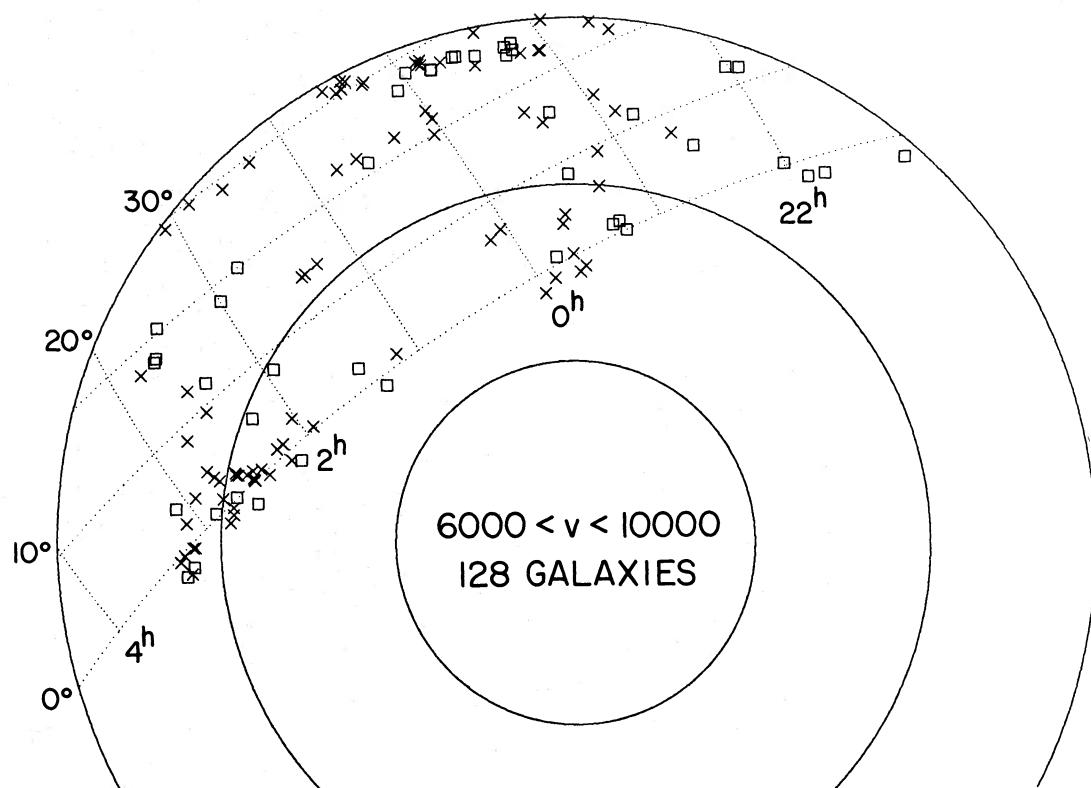
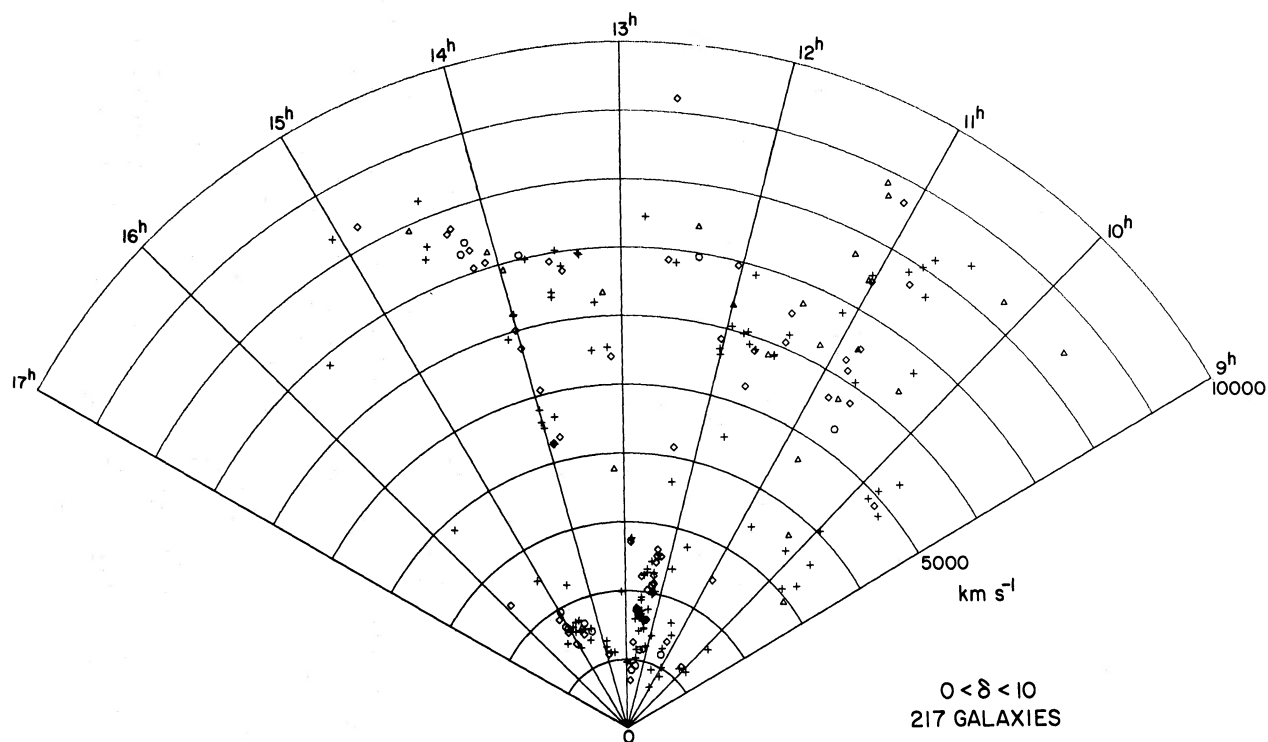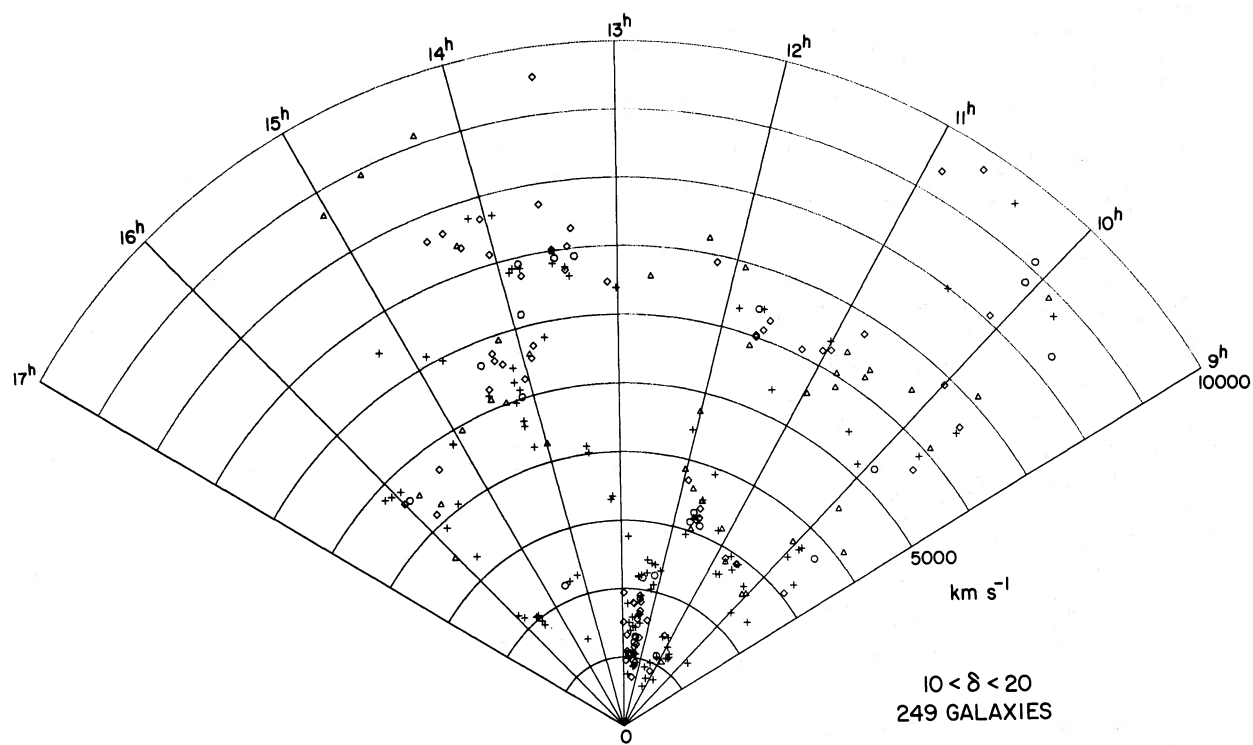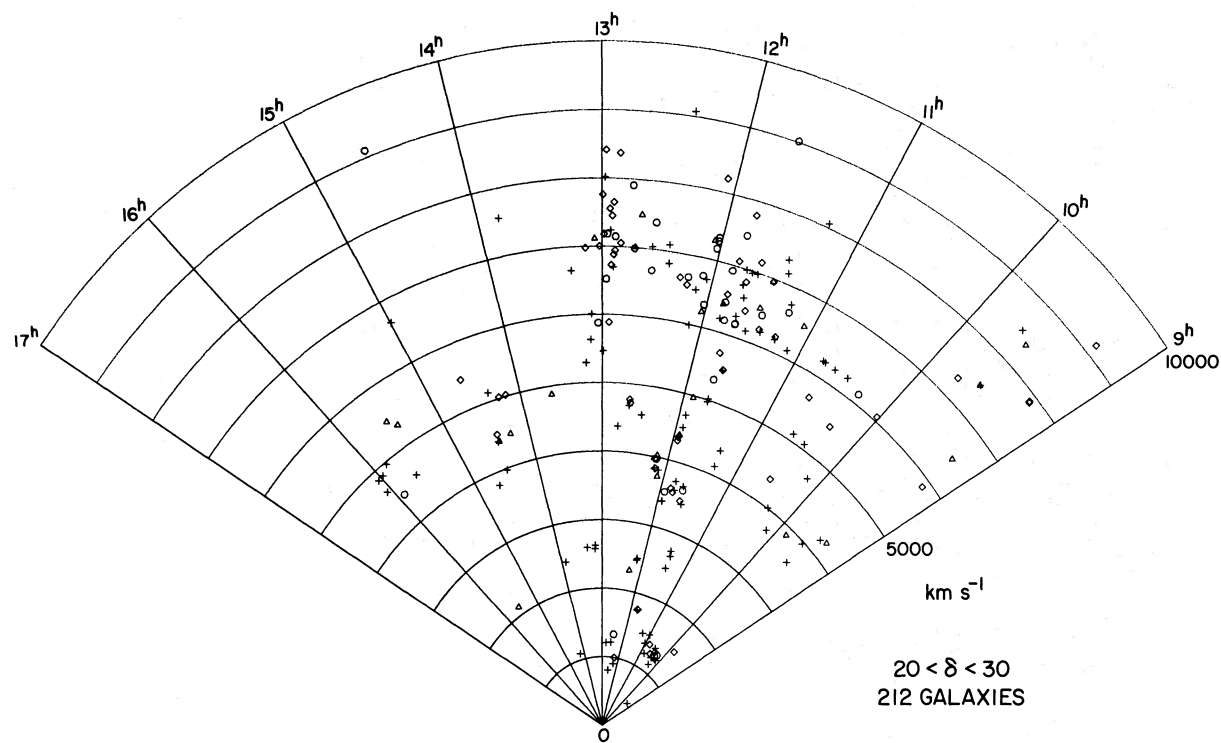FIG. 3c.—Same as Fig. 3a for galaxies in the range $6000 < v < 10{,}000$ km s^{-1}

FIG. 4a.—A transverse map of the northern cap survey with observed velocity plotted versus right ascension for different wedges of declination. Compare to Fig. 2 for orientation. All galaxies shown are selected to have $M < -18.5$ and are in the velocity range $0 < v < 10{,}000$ km s^{-1}. The different symbols denote morphological type generally as listed by Nilson (1973). Circles are ellipticals, diamonds denote SOs, pluses are spirals, and triangles are irregulars. This figure shows the declination wedge $0 < \delta < 10°$.

431

FIG. 4b.—Same as Fig. 4a for declination wedge 10° < δ < 20°

FIG. 4c.—Same as Fig. 4a for declination wedge 20° < δ < 30°

432

Fig. 4d.—Same as Fig. 4a for declination wedge $30° < \delta < 40°$

Fig. 4e.—Same as Fig. 4a for declination wedge $40° < \delta < 50°$

433

FIG. 4f.—Same as Fig. 4a for declination wedge $50° < \delta < 60°$

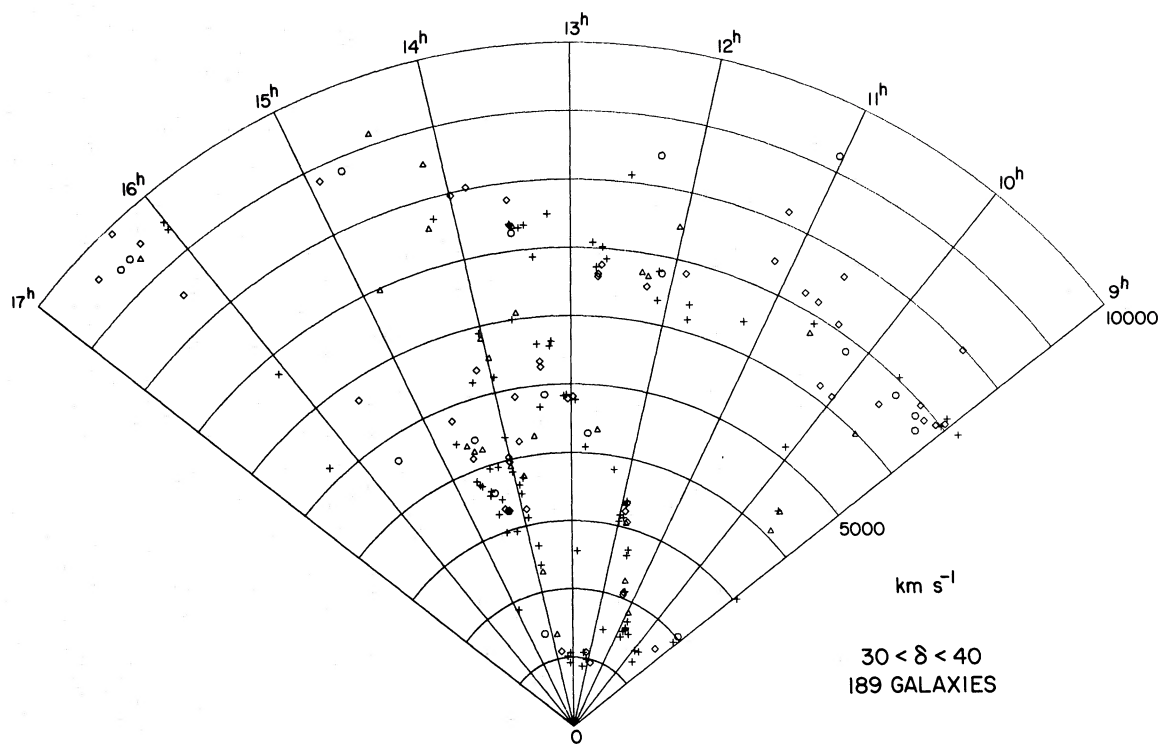FIG. 4g.—Same as Fig. 4a for declination wedge $60° < \delta < 80°$

434

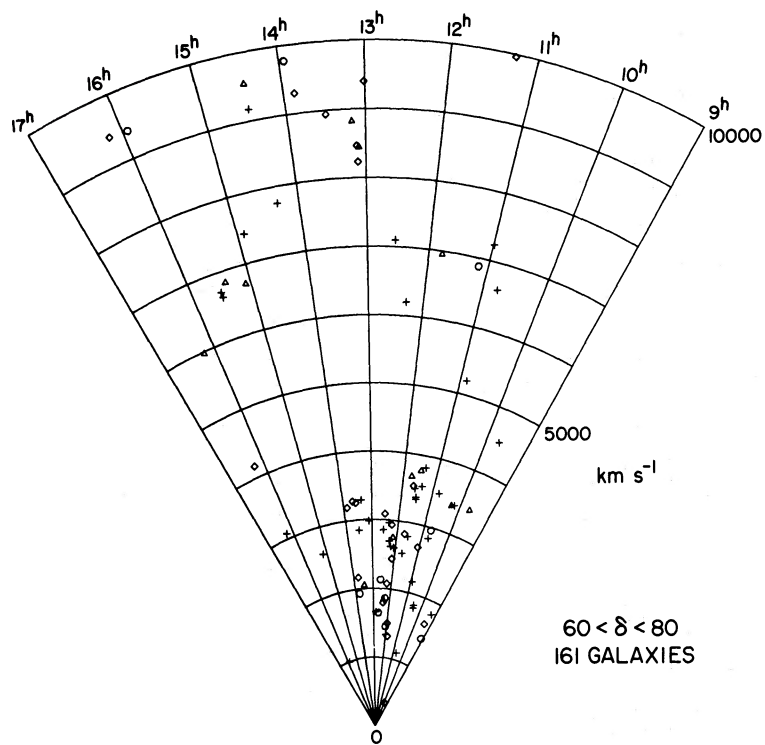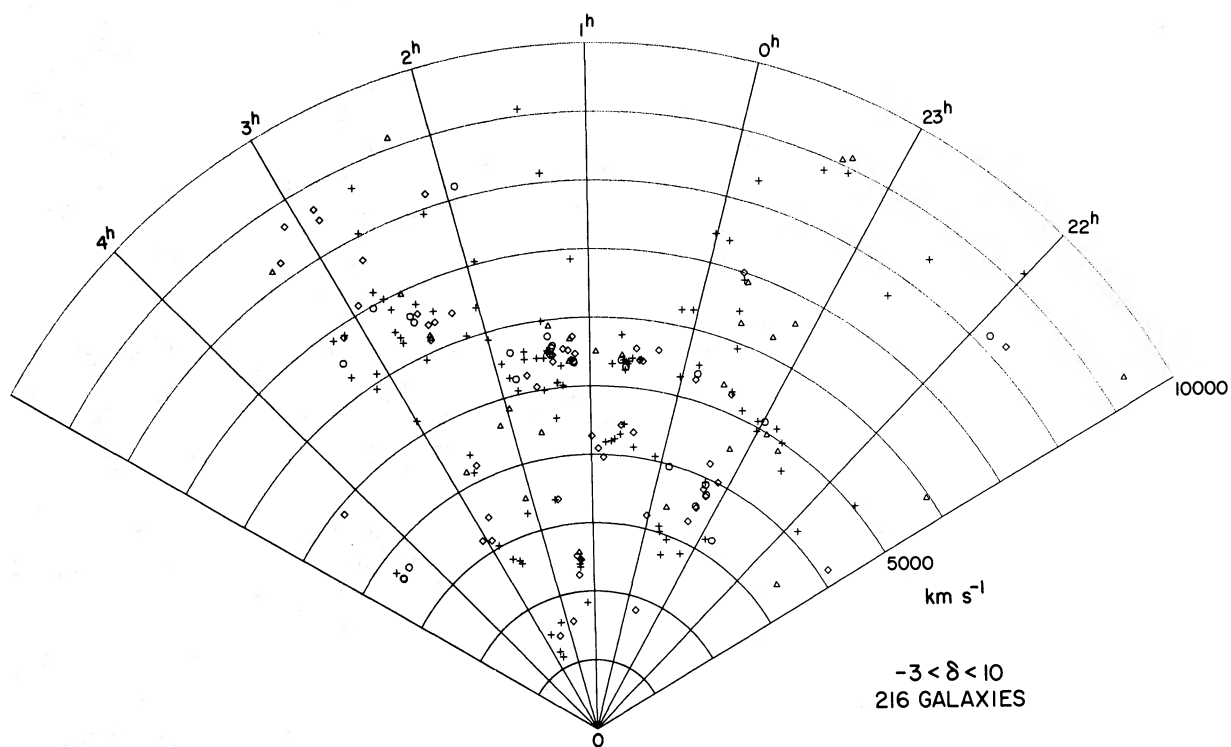FIG. 5a.—A transverse map of the southern galactic survey. The selection procedures and symbols are the same as those in Fig. 4a. This figure shows the declination wedge $-3° < \delta < 10°$.

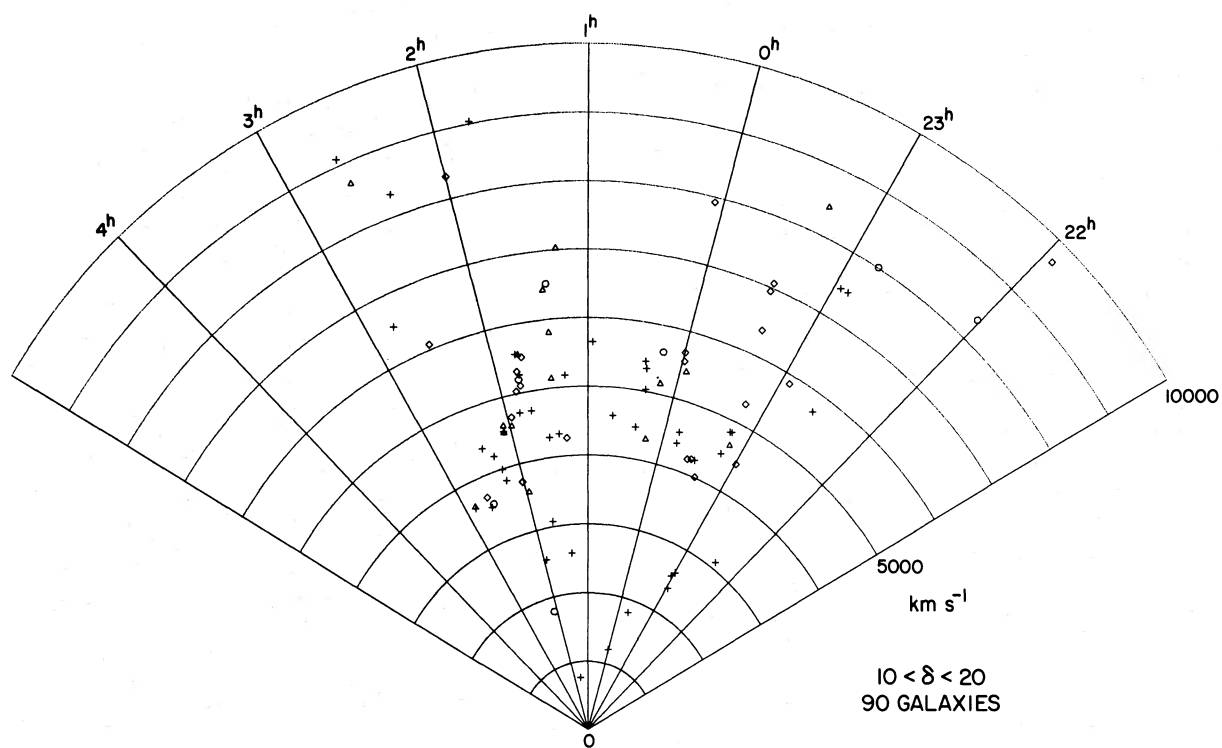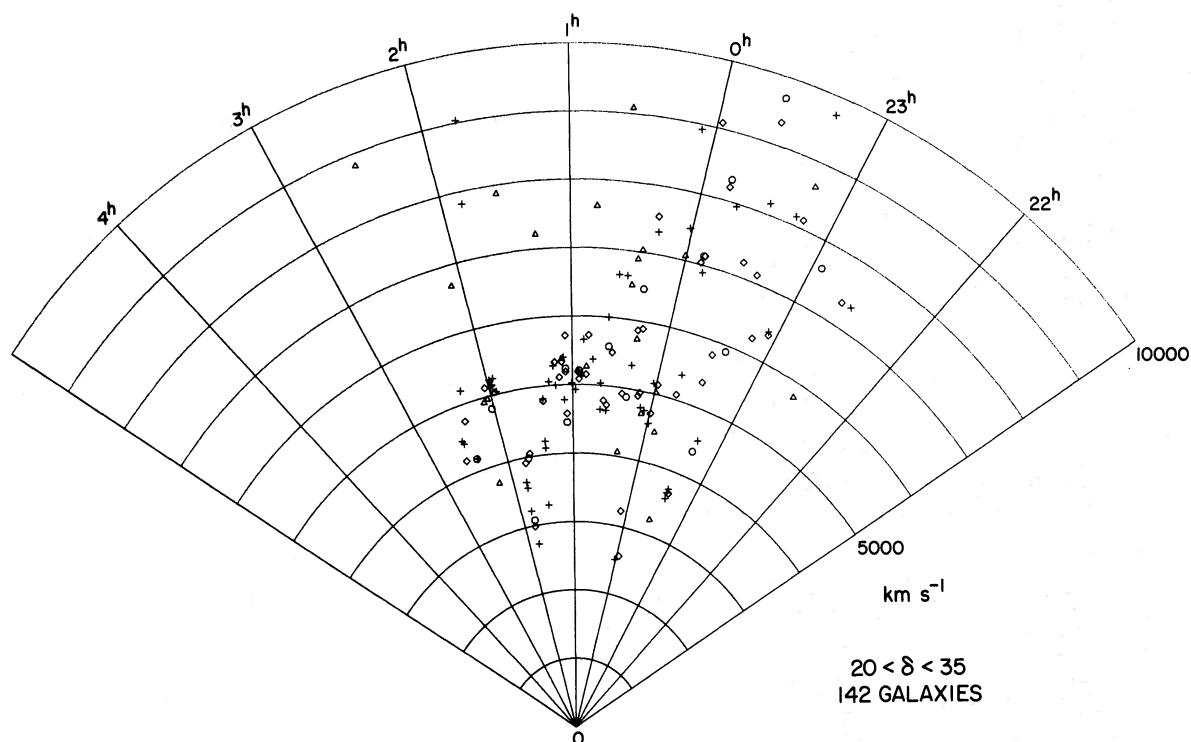FIG. 5b.—Same as Fig. 5a for declination wedge $10° < \delta < 20°$

435

FIG. 5c.—Same as Fig. 5a for declination wedge $20° < \delta < 35°$

little or no connection with any well defined "supercluster." There is much of the distribution that appears to be quite random on large scale.

Equally prominent with the clusters are the large empty holes, as much as 30 Mpc in diameter. A good example is the hole near the Coma cluster and centered at $(14^h5, +30°, 7000$ km s$^{-1})$ where a spherical volume of diameter ~ 30 Mpc would include only 20 galaxies from the survey. This large region has a space density of roughly 20–30% of the mean of our sample. Numerous other holes are equally prominent, such as one behind the Virgo cluster $(12^h5, +12°, 5000$ km s$^{-1})$ and another at $(14^h, +60°, 6000$ km s$^{-1})$.

The redshift-space maps can be distorted by virial motion in cluster centers as obviously seen for a few of the richer clusters, but they can be additionally distorted by the coherent infall of outlying galaxies to cluster centers, which flattens the cluster image in the velocity dimension. This effect is more difficult to identify but is perhaps occurring in the southern agglomeration of clusters, mentioned above, which is slightly flattened in the velocity dimension. Another candidate cluster for this effect is the loose association centered roughly at $(14^h1, +10°, 7000$ km s^{-1}, the NGC 5416 group) which appears to be a flattened disk tilted slightly to the line of sight. Coherent infall will also elongate redshift-space holes in the velocity direction, but no unambiguous examples of this are apparent.

All these remarks are intended to be taken in a qualitative spirit. The subdivision of this sample space into individual groups will be discussed by Huchra and Geller (1981) and by Press and Davis (1981). The notion of chains defining cell boundaries has been discussed extensively by Einasto, Joêver, and Saar (1980 and references therein), especially for the Perseus supercluster. To our eyes, it is relatively easy to identify linear structures in the large scale distribution, but very difficult to identify planar structures. This could be a perception problem, and it is a difficult issue to quantify.

III. COMPARISON TO SIMULATIONS

A comparison of the observed distribution to n-body simulations is quite illuminating. We have used a snapshot of a 20,000 body simulation kindly given to us by George Efstathiou and discussed in Efstathiou and Eastwood (1981). This simulation is an $\Omega = 1$ model run in an expanding periodic cube. To generate from this a sample that is apparent magnitude limited, we scale the cube to a size of 150 Mpc and position the observer in a corner. Because this simulation has a time behavior that appears to be self-similar, any time slice of the simulation should be useable. The snapshot supplied to us was at an expansion factor of 9.9 from an initial random distribution. Our choice of length scale was dictated by
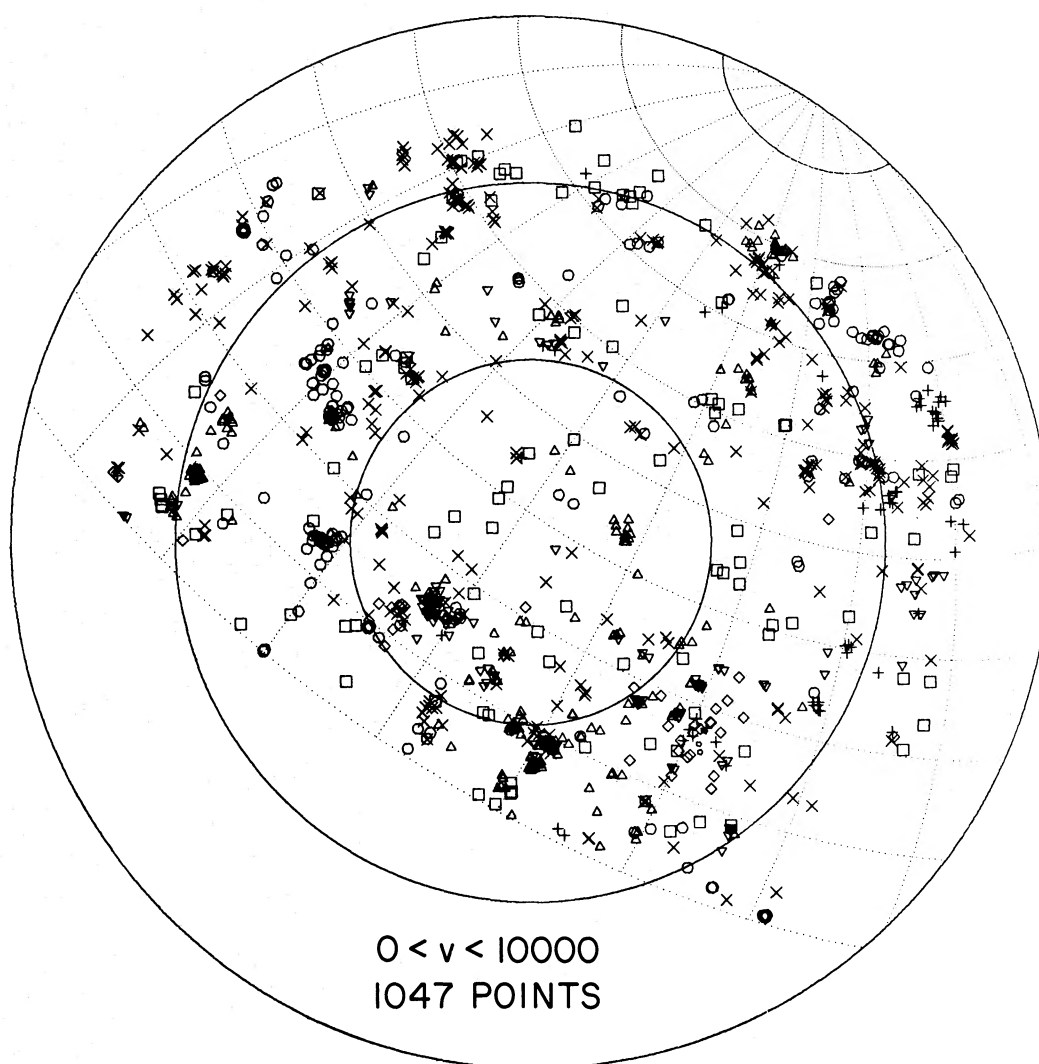
FIG. 6a.—A sky projection of the n-body simulation of Efstathiou and Eastwood (1981). The selection procedure is described in the text. This projection shows all points in the range $0 < v < 10,000$ km s^{-1}. The symbols are the same as those in Fig. 1.

the desire to match the galaxy correlation length r_c [$\xi(r_c) = 1$] to the observations, where $r_c \sim 5$ Mpc. Fortunately, this resulted in a near match to the observations of an important dimensionless quantity: the number of particles (or galaxies) in one clustering (or coherence) length. Existing simulations for $\Omega < 1$ unfortunately do not have sufficient objects per coherence length to compare to the observations.

Since few galaxies in our sample are more distant than 100 Mpc, we do not strain the periodicity of the simulation. Each point in the simulation is assigned a luminosity randomly drawn from the luminosity distribution function observed in the northern sample (to be discussed in Paper III) and only points with apparent $m_B < 14.5$ are retained. The minimum luminosity of a point is $M = -18.5$, so the sample will again be

volume-limited to 4000 km s^{-1}. For the simulation we of course know all six degrees of freedom for each point, so we can generate an observable velocity $v_0 = H_0 l + K v_p$, where l is the distance to the object, v_p is the component of random thermal motion of the object projected in the line of sight, and $K = 1/3$ is a scale factor applied to all the objects. To be completely self-consistent in this $\Omega = 1$ simulation, we should use $K = 1$, but this would produce too much elongation of the clusters compared to the observed distribution. By setting $K = 1/3$, the RMS one-dimensional random motion of points in the simulation is 350 km s^{-1}. If all points were in virialized clusters, then the cosmological density approximately scales as $\Omega = K^2$, but since the simulation is evolving on dynamical timescales, our use of $K = 1/3$ is not quite self-consistent. It would be
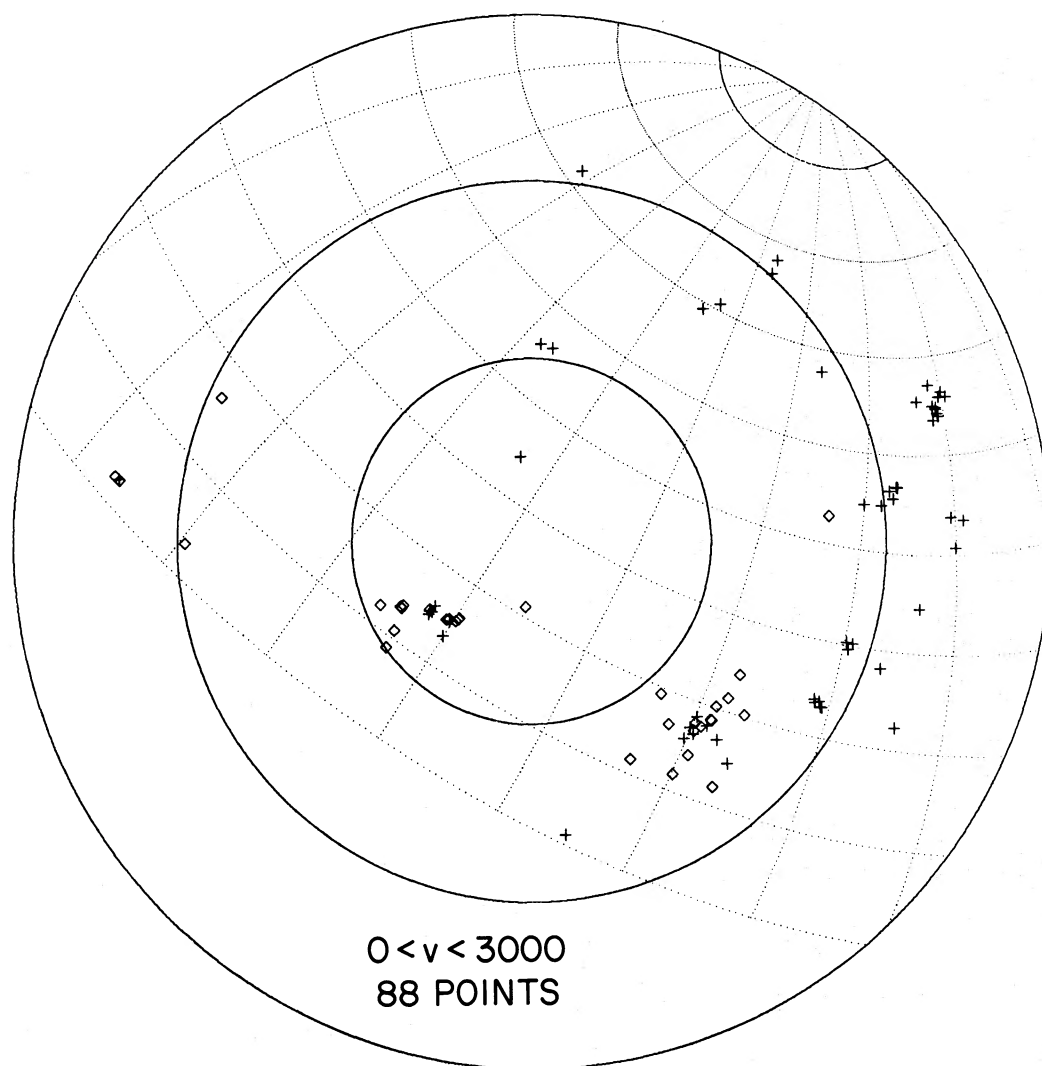
FIG. 6b.—Same as Fig. 6a for points in the range $0 < v < 3000$ km s^{-1}

preferable to use a $\Omega < 1$ simulation for comparison to the observations, but again, existing $\Omega < 1$ simulations are only weakly clustered and do not begin to approximate the observed distributions.

Figures 6a, 6b, 6c, and 6d show the resulting simulation catalog when projected onto the sky, and Figures 7a, 7b, 7c, and 7d show R.A.-v projections for selected slices of declination. Although the space density of objects and correlation length of clustering is roughly the same in the two samples, there are obvious glaring differences between the n-body catalog and the observed catalog.

The simulation is characterized by very prominent dense cluster centers with pronounced elongation in redshift space, but no large scale connectedness among the clusters. The size and distribution of holes in redshift space is similar in the two samples. If K were further reduced, the elongation of the clusters would shrink but the cluster centers would be too dense.

Although Figures 2b and 6c bear essentially no resemblance to each other, Figures 2c and 6d are quite similar. This is because these projections are at sufficient distance that 10° corresponds to projected separation greater than 10 Mpc, a scale on which $\xi(r) < 1$, so that both maps are relatively weakly clustered. The rapidly falling selection function at this distance also dilutes the details of the observed clustering. This is especially apparent in Figure 7 where for large distance the cluster definition is less distinct than for smaller distance. If our sample were 0.5 mag deeper, we would more clearly define structures and holes beyond 7000 km s^{-1}, which now are somewhat ambiguous.
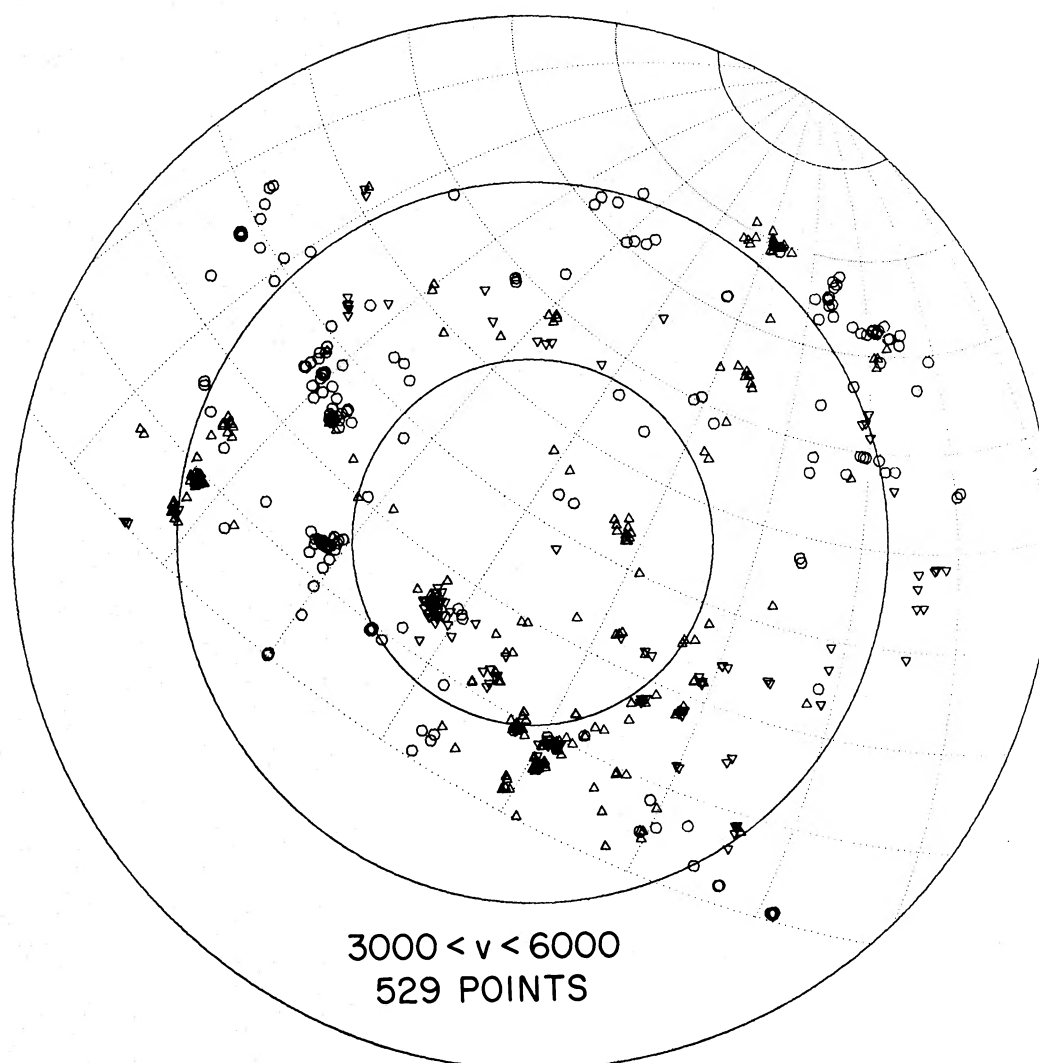
3000 < v < 6000
529 POINTS

FIG. 6c.—Same as Fig. 6a for points in the range $3000 < v < 6000$ km s^{-1}

The obvious difference in the nature of the clustering between the observations and the simulations also is evident in their correlation functions. Although this will be discussed in detail in a future paper, we comment here only that $\xi(r)$ for the observed distribution is well described by a power law of slope -1.8 for $r < 5$ Mpc, whereas $\xi(r)$ for the simulation is not well matched by a power law and is a continuously steepening function with an average power law slope of -2. Efstathiou's n-body simulations do, however, have a covariance function that closely matches the 1000 body simulations of Aarseth, Gott, and Turner (1979).

IV. DISCUSSION

The CfA redshift survey complements those previous deeper surveys that focused on relatively small fields around nearby rich clusters. We now have a detailed three-dimensional view over 2.7 sr that reaches to a depth which includes several rich Abell clusters. It is clear that strong clustering on a scale of up to 20 Mpc is the rule and that holes of 20–30 Mpc in diameter are quite common, with the observed clusters seemingly quite extended and connected. The boundaries of the very empty holes are defined by the connections, or filaments, between richer clusters, the topology of which is obviously complex. One must speak rather loosely about holes and filaments, but they are inextricably woven together.

An important point is to consider how well this survey approaches a "fair sample" volume of the universe. One can never be certain that a single given volume is a fair sample of some ensemble, and it is not entirely clear whether the universe is homogeneous
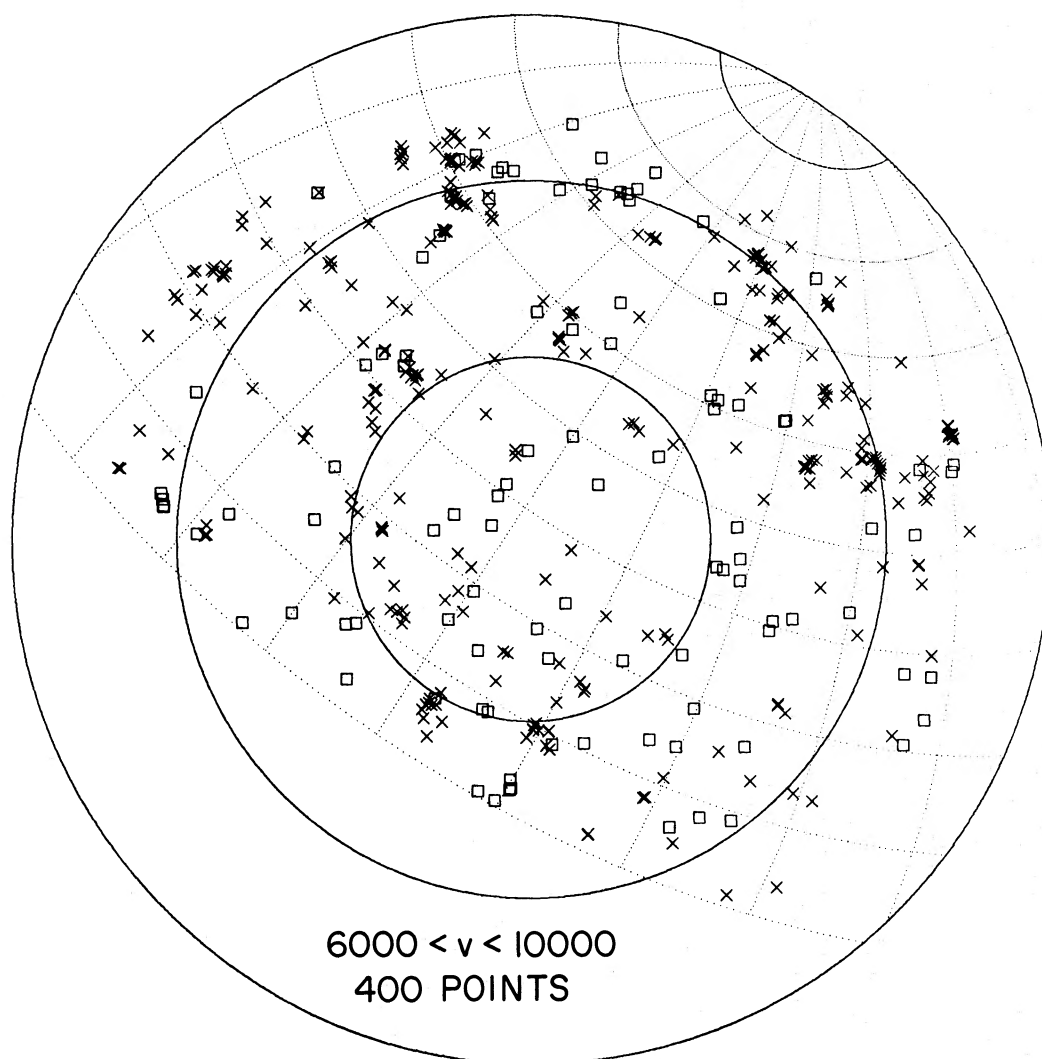
6000 < v < 10000
400 POINTS

FIG. 6d.—Same as Fig. 6a for points in the range $6000 < v < 10,000$ km s^{-1}

enough for a fair sample volume to exist on scales less than several hundred Mpc. The obvious test is to intercompare two independent subsamples: if they are each fair samples, they will have similar average densities and statistical properties, but having similar properties obviously does not imply that the two samples are necessarily fair representations of the parent ensemble. When one intercompares the maps of our northern sample with the independent southern sample, there is a very similar filamentary appearance not reproduced in the n-body maps. The northern sample is overdense in the foreground and background, and underdense in the 3000–6000 km s^{-1} region; exactly the opposite is true in the southern sample. Fluctuations of 30 Mpc scale length apparently are real and are sampled adequately (but barely) in our survey. In Paper III of this series (Davis and Huchra 1981) we show that the mean number

density of bright galaxies ($M < -18.5$) agrees within 7% between the northern and southern samples, an event unlikely to occur if very large scale fluctuations (>50 Mpc) dominate the distribution. Thus there is some evidence that we are beginning to reach to a fair sample volume in which dynamical inferences can be applied to the universe at large.

Our view of the large scale universe has recently undergone considerable evolution. A few years ago Abell clusters were considered as isolated rare islands of high density in an otherwise uniform background field of galaxies, which themselves were largely clustered into small groups. Now it is apparent that there is essentially no "field" component and that the clusters have such a large extent that it is impossible to define where one ends and the next begins. Nearly all of the galaxies in this sample are highly clustered on small scales, so

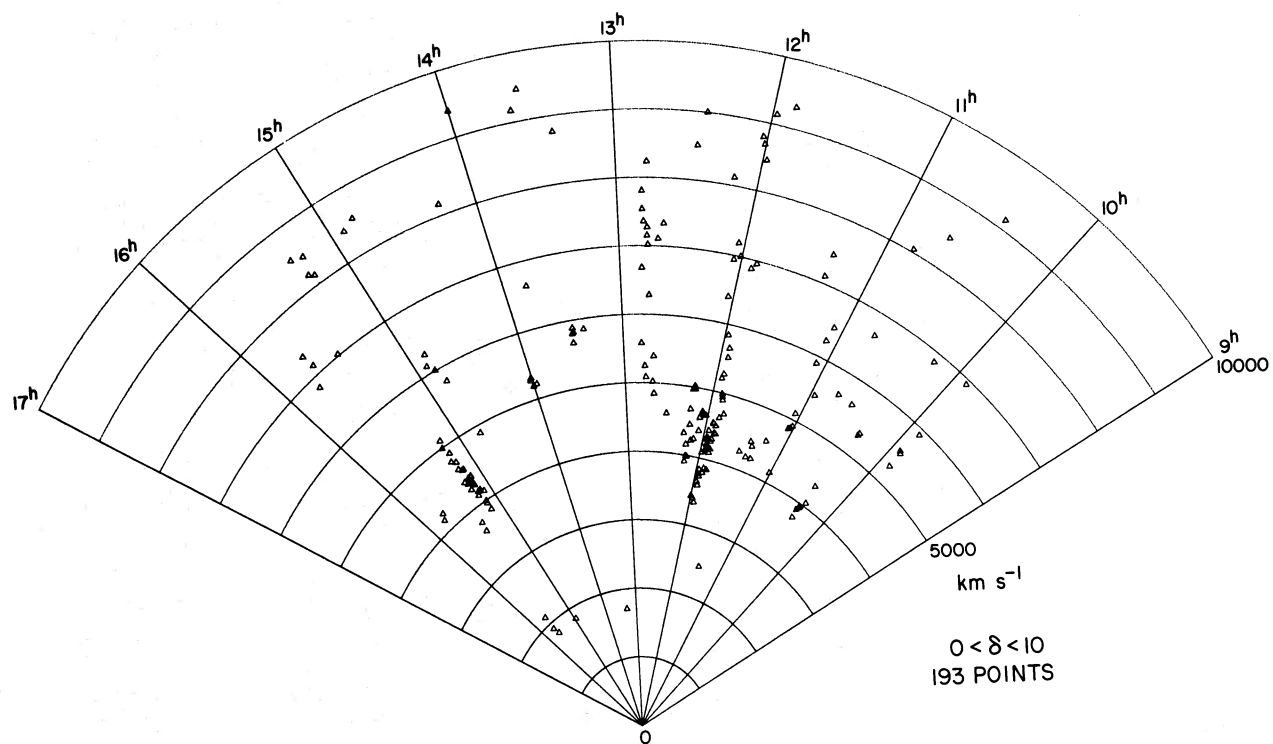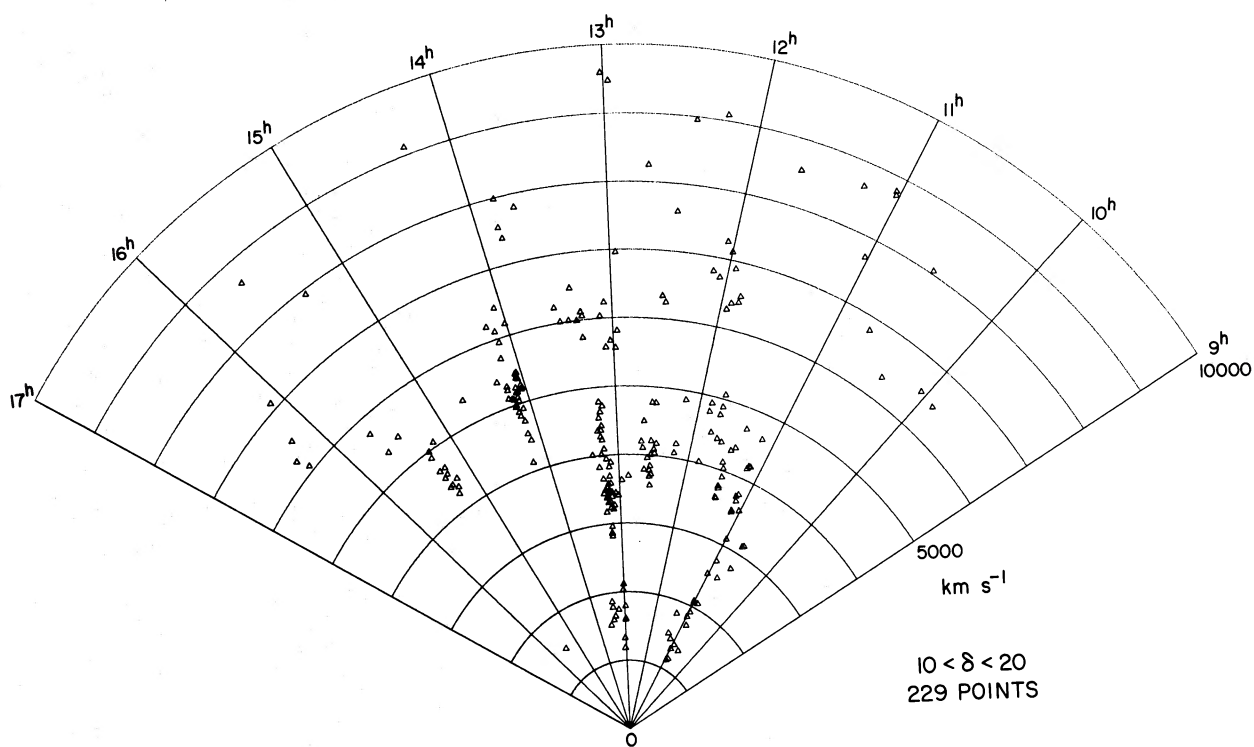Fig. 7a.—A transverse right ascension-velocity map of the n-body simulation for the wedge of declination $0° < \delta < 10°$
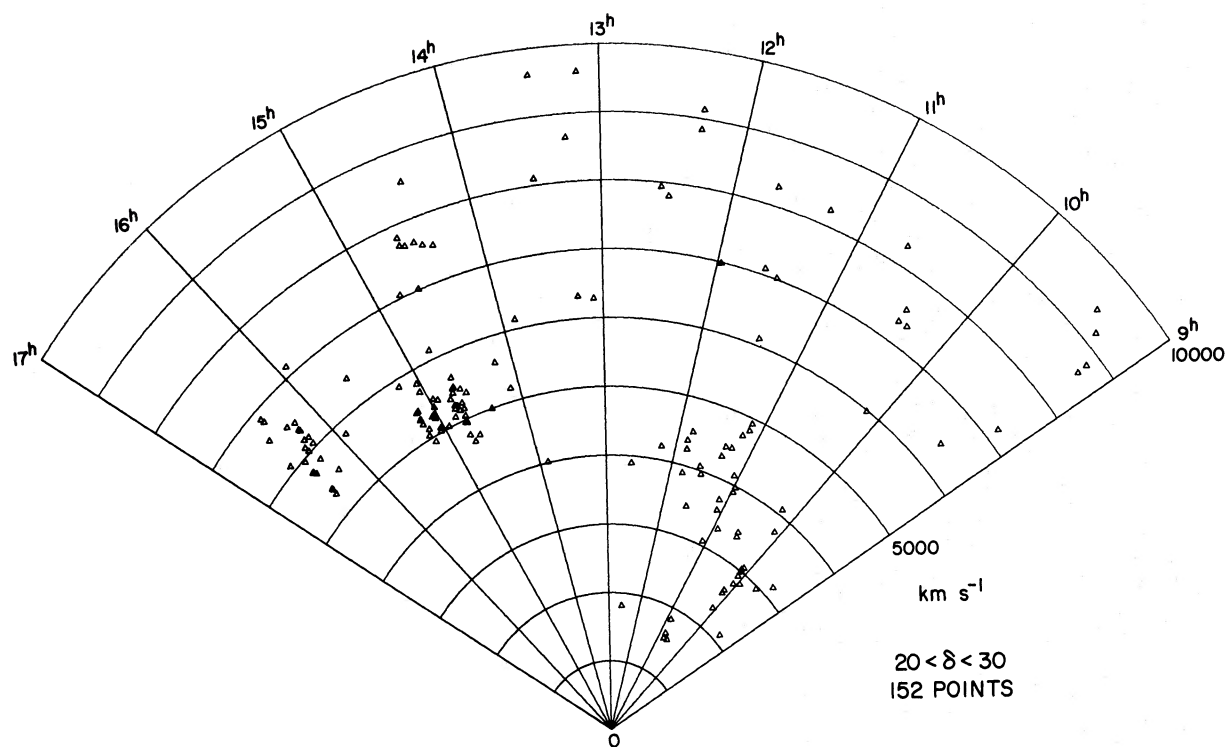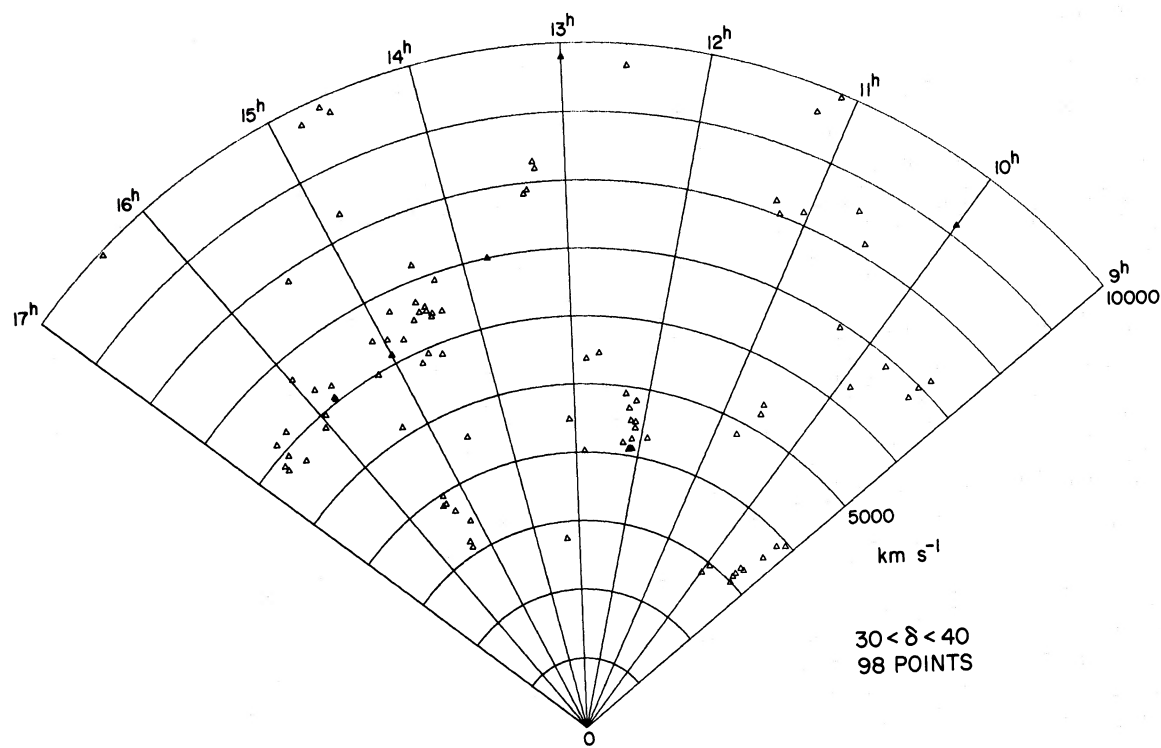

Fig. 7b.—Same as Fig. 7a for declination wedge $10° < \delta < 20°$

FIG. 7c.—Same as Fig. 7a for declination wedge $20° < \delta < 30°$

FIG. 7d.—Same as Fig. 7a for declination wedge $30° < \delta < 40°$

almost by definition there must exist large zones of less than average galaxy density.

The emerging picture presents a severe challenge to all theories of cluster formation and evolution. If we suppose that the present highly irregular distribution arose from an earlier, more uniform universe, then we must explain how a typical lump of matter has moved a distance of ~ 10–20 Mpc in one Hubble time. Of course, this presupposes that the matter and light distributions are highly correlated, which may be totally in error and can only be true in some very large scale average (Davis *et al.* 1980).

If one were to suppose that the gravitational instability scenario (Peebles 1980) were totally responsible for all systems larger than galaxies, then galaxies are the seeds which congregate through their own self-gravity into clusters and groups. The *n*-body simulations should include all the essential physics of this process, and yet they fail to mimic the observed distribution in any real sense. Is this because some additional physical process, such as dissipation, has been left out? Or perhaps it is necessary to use a two fluid model to simulate the universe, one component of which can dissipate energy and the other cannot. Perhaps the initial conditions did not properly match those of the early universe. At present the *n*-body experiments are limited to white noise initial conditions, whereas the initial spectrum of perturbations in the universe is only a conjecture. The *n*-body experiments do show substantial holes in redshift space and the particles have random thermal velocities high enough (if $K = \Omega = 1$) to have made these holes in one Hubble time. In the actual distribution, the random velocity field seems to be much smaller (this point will be addressed in detail in a later paper), which would seem to argue against the gravitational instability picture in a high Ω universe.

For example, suppose that the holes in redshift space are devoid of matter. Then to produce the 20 Mpc diameter holes so conspicuous in the observed distribution, a typical galaxy would have moved ~ 10 Mpc in one Hubble time. In expanding coordinates with $a(t)$ the expansion parameter, the physical distance an object has traveled to the present time t_0 is simply

$$d(t_0) = a_0 \int_0^{t_0} \frac{v(t') \, dt'}{a(t')}, \qquad (1)$$

where $v(t)$ is the non-Hubble velocity induced by inhomogeneities in the matter distribution.

In an Einstein-de Sitter universe, $\Omega = 1$, $a(t) = a_0(t/t_0)^{2/3}$, and peculiar velocities induced by the growing mode of linear perturbations have a time behavior $v(t) = v_0(t/t_0)^{1/3}$ (cf. Peebles 1980), in which case $v_0 = [2d(t_0)/3t_0] = H_0 d(t_0)$. Thus 10 Mpc motion requires peculiar velocities of 1000 km s^{-1} today (independent of the value of H_0), which seems high. The

peculiar motion of our own galaxy is probably less than 600 km s^{-1}, and only the virial velocity in rich clusters of galaxies approaches this number. This velocity is not too high for the *n*-body simulations, if we had allowed $K = 1$. However, these peculiar motions are expected to have a coherence length of 5–10 Mpc, and they will not necessarily result in conspicuous redshift elongation on larger scales. Quite the opposite is likely because these are the unvirialized regions where the redshift dimension of a cluster can be flattened by the infall of outer regions.

The above simple result can be readily generalized to an open universe $\Omega < 1$. If the time behavior of the growing mode perturbation is $D_1(t)$, then the associated peculiar velocity varies as $v(t) \propto a(t)(dD_1/dt) = H(t)a(t)(dD_1/da)$ (Peebles 1981, p. 64; Groth and Peebles 1975). From equation (1) we therefore have $d(t) \propto a(t) D(t)$, and

$$v(t) = d(t)H(t)f(\Omega), \quad f(\Omega) = \frac{a(t)}{D_1}\frac{dD_1}{da} \approx \Omega^{0.6},$$

$$(2)$$

and

$$v_0 = d_0 H_0 \Omega^{0.6}. \qquad (3)$$

This simple result is strictly true only for small perturbations, whereas observed galaxy clusters are fluctuations of order unity. Even if the universal Ω is as low as 0.1, which is the lowest value acceptable from the Virgocentric flow problem (Yahil 1980) the local, effective Ω to use for equation (3) cannot be much lower than $\Omega_{eff} \sim 0.3$. This in turn leads to $v_0 \sim 450$ km s^{-1}, still a very high value. For reasonable estimates, $0.1 < \Omega < 0.5$, the universe is not very different from being closed, and the redshift space maps should continue to show high random velocities.

We are not suggesting that the standard gravitational instability scenario is incompatible with the data, but the scenario is definitely strained, and more detailed simulations and models should be performed.

Alternative theories of cluster formation such as those of Zeldovich (1978), Zeldovich and Novikov (1975), or Ostriker and Cowie (1981) involve dissipative processes and so could in principle more readily explain large holes and not so large random velocities simultaneously. If the mysterious dark matter in halos and binding clusters of galaxies is itself dissipationless, then dissipational formation of galaxies would provide a natural mechanism for the separation of the luminous galaxies from their dark halos and could partially explain the observed trend of M/L ratios with system scale size (Ostriker, Peebles, and Yahil 1974; Einasto, Kaasik, and Saar 1974; Davis *et al.* 1980). In the pancake model

favored by Zeldovich and collaborators, the initial systems to collapse are very massive, and the danger is that the separation of the dissipationless halo and the dissipational galaxy will be so violent and complete that galaxies will be unable to retain the $1/r^2$ dark halo that they all seem to possess. In addition, existing pancake simulations which do somewhat match the observed filamentary distribution of the galaxy clusters (Doroshkevich *et al.* 1980*b*) have been two-dimensional, and it is not obvious that a full three-dimensional simulation would equally well mimic the observations. There are few obvious pancakes in the observed distribution; the Virgo supercluster is probably typical of most rich regions, and it is not strongly oblate.

In the pancake models, galaxy formation occurs dissipatively *after* the pancake collapse. With the increasing possibility that cosmological neutrinos have finite rest mass and could dominate the mass density of the Universe, the size of the initial pancakes is very large, $>4 \times 10^{15}$ $M_\odot$ (Doroshkevich *et al.* 1980*a*). This is a mass typical of an entire supercluster like Virgo, and these systems are just beginning to collapse today, not at $Z \sim 5$, the lowest reasonable redshift of galaxy formation.

Again, this cosmogonic scenario is highly strained by the observations, and extensive model studies must be performed to determine its viability.

In the collective explosion model of Ostriker and Cowie (1981), supernovae in massive stars at epoch $Z > 5$ form snowplow shells which quickly cool, fragment, and gravitationally collapse. The procedure cascades upward in scale until the shells are unable to cool in one Hubble time. The resulting matter distribution consists of cool clouds embedded in a hot intergalactic plasma. The clouds fragment to form small groups of galaxies with low velocity dispersion, and holes of up to 100 Mpc radius are possible. Furthermore, unvirialized systems are expected to lie on two-dimensional surfaces. This scenario appears at least as consistent with the observed distribution as the above mentioned alternatives. Whether this model is capable of describing the variety and hierarchical nature of the observed clustering is uncertain. The expected unvirialized sheets of matter are not present, and the filaments

have a width more like 10 Mpc rather than 2 Mpc. The model is in a preliminary form, and much work must be done before a judgment on its viability can be reached.

V. CONCLUSION

We have presented a series of projections of the galaxy distribution as seen to a limiting Zwicky magnitude of 14.5. This sample reaches a substantial depth, and the volume surveyed encompasses numerous holes, rich clusters, and filaments. Future papers in this series will discuss some quantitative aspects of the distribution. Our purpose here is to provide inspiration to all model builders interested in simulating the large scale structure of the universe. We caution the reader to note that our catalog is magnitude limited, and our pictures are semivolume limited to a Hubble velocity of only 4000 km s^{-1}. The steep slope of the bright end of the galaxy luminosity function imposes a strong selection function against galaxies much beyond a distance of 8000 km s^{-1}, so it is not clear how real the holes behind the Coma/A1367 clusters are.

That the general nature of the clustering appears so similar in the north and south galactic caps is encouraging and suggests that the large scale universe does obey some well defined statistical law. We believe it is safe to say that we do not as yet have a full understanding of the processes involved. Observations are now extensive enough to challenge present theories of the formation and structure of the large scale distribution of matter, and the resolution of this challenge is likely to occupy the attention of cosmologists and particle physicists for some years to come.

REFERENCES

Aarseth, S.J., Gott, J.R., and Turner, E.L. 1979, *Ap. J.* **234**, 13.
Chincarini, G., Haynes, M., and Giovanelli, R. 1979, *A. J.*, **84**, 1500.
Davis, M., and Latham, D. W. 1979, in *Proc. Soc. Photo-Opt. Instrum. Eng.*, **172**, *Instrumentation in Astronomy III*, 11.
Davis, M., and Huchra, J. 1981, *Ap. J.*, submitted (Paper III).
Davis, M., Tonry, J., Huchra, J., and Latham, D. 1980, *Ap. J. (Letters)*, **238**, 113.
de Vaucouleurs, G., and de Vaucouleurs, A. 1973, *Astr. Ap.*, **28**, 109.
Doroshkevich, A. G., Khlopov, M. Y., Sunyaev, R. A., Szalay, A. S., and Zeldovich, Y. B. 1980*a*, in 10th Texas Symposium on Relativistic Astrophysics.

Doroshkevich, A. G., Kotok, E. V., Novikov, I. D., Polyudov, A. N., Shandarin, S. F., and Sigov, Y. S. 1980*b*, *M.N.R.A.S.*, **192**, 321.
Efstathiou, G., and Eastwood, J. W. 1981, *M.N.R.A.S.*, **194**, 503.
Einasto, J., Joêver, M., and Saar, E. 1980, *Nature*, **283**, 47.
Einasto, J., Kaasik, A., and Saar, E. 1974, *Nature*, **250**, 309.
Ellis, R. A., *et al.* 1981, in preparation.
Gregory, S. A., and Thompson, L. A. 1978, *Ap. J.*, **222**, 784.
Gregory, S. A., Thompson, L. A., and Tifft, W. G. 1981, *Ap. J.*, **243**, 411.
Groth, E. J., and Peebles, P. J. E. 1975, *Astr. Ap.*, **41**, 143.
Huchra, J., and Geller, M. J. 1981, in preparation.
Kirshner, R., Oemler, A., and Schechter, P. 1979, *A.J.*, **84**, 951.

Nilson, P. 1973, *Uppsala Astr. Obs. Ann.*, **6** *Uppsala General Catalogue of Galaxies*.
Ostriker, J. P., and Cowie, L. L. 1981, *Ap. J.* (*Letters*), **243**, L127.
Ostriker, J. P., Peebles, P. J. E., and Yahil, A. 1974, *Ap. J.* (*Letters*), **193**, L1.
Peebles, P. J. E. 1980, *The Large Scale Structure of the Universe* (Princeton, N.J.: Princeton University Press).
Press, W., and Davis, M. 1981, *Ap. J.*, submitted.
Rood, H. J. 1981, preprint.
Sandage, A. 1978, *A.J.*, **83**, 904.
Tarenghi, M., Chincarini, G., Rood, H. J., and Thompson, L. A. 1980, *Ap. J.*, **235**, 724.
Tarenghi, M., Tifft, W. G., Chincarini, G., Rood, H. J., and Thompson, L. A. 1979, *Ap. J.*, **234**, 793.
Thompson, L., Wellier, W., and Gregory, S. 1978, *Pub. A.S.P.*, **90**, 644.

Tifft, W. G. 1980, *Ap. J.*, **239**, 445.
Tonry, J. 1980, Ph.D. thesis, Harvard University.
Tonry, J., and Davis, M. 1978, *A.J.*, **84**, 1511 (Paper I).
———. 1981*a*, *Ap. J.*, **246**, 666.
———. 1981*b*, *Ap. J.*, **246**, 680.
Tully, R. B., and Fisher, R. 1981, preprint.
Yahil, A. 1980, in the 10th Texas Conference on Relativistic Astrophysics.
Zeldovich, Y. B. 1978, in *IAU Symposium 79, The Large Scale Structure of the Universe*, ed. M. S. Longair and J. Einasto (Dordrecht: Reidel), p. 409.
Zeldovich, Y. B., and Novikov, I. D. 1975, *Structure and Evolution of the Universe*, Moscow.
Zwicky, F., Herzog, E., Wild, P., Karkowicz, M., and Kowol, C. 1961, *Catalog of Galaxies and of Clusters of Galaxies*, Vols. **1–6** (Pasadena, Cal.: California Institute of Technology).

MARC DAVIS, JOHN HUCHRA, and DAVE LATHAM: Center for Astrophysics, 60 Garden Street, Cambridge, MA 02138

JOHN TONRY: Institute for Advanced Study, Princeton, NJ 08540